Comments for the Reviewers

We thank the reviewers for the positive and constructive comments. The author responses are in blue.

Late reviewer comments.

Reviewer comment: My remaining criticism, which would still lead to rejection for me (or contengency on the publication of their Nature Comms paper), is that the mechanism still not listed in their revision. Moreover, of the 2 references they have stated are in the bibliography that describe PRAM in detail, the Öström one is incomplete and the Ximeng one is missing. I did find a PRAM model listing in Emilie Öström's thesis online (https://portal.research.lu.se/portal/files/31835271/Emilie_str_m_hela_inkl._omslag.pdf), but it does not seem to correspond to what is in the current Xavier et al. paper, and paper III in the thesis may refer to an old version of what later became the Nature Comms submission. I do not feel that the model description in sufficient to allow publication with the current existing confusion.

Thank you for being patient. The Nature Communications paper by Roldin et al., 2019 has now been accepted for publication and will be published on 25th September 2019. In this paper there is a link provided to download the complete PRAM mechanism written in a format compatible with the Kinetic PreProcessor (KPP) together with all species information [https://doi.org/10.1594/PANGAEA.905102]. Also the reference to Roldin et al., 2019 will be updated in case this paper has been successfully accepted.

This information is also provided in this paper under 'Data availability' in the end of the paper as following text:

The complete PRAM mechanism written in a format compatible with the Kinetic PreProcessor (KPP) together with all species information can also be downloaded from https://doi.org/10.1594/PANGAEA.905102

Reviewer 1

This paper presents a study of the SOA-forming potential of autoxidation mechanisms for several important BVOCs, as expressed in the PRAM chemical mechanism. A suite of box model simulations is performed for both chamber and OFR conditions using the MCM alone and in combination with PRAM. SOA yields simulated using MCM+PRAM show significantly better agreement with experimental data than do the MCM-only simulations, indicating the importance of the autoxidation reactions included in PRAM to

SOA production. Sensitivity studies are also presented showing of the influence of temperature and NO variations on the contribution of the autoxidation mechanism to the overall SOA yield. This appears to be a careful and comprehensive study, and is a valuable contribution to the literature. I recommend publication after the following points have been addressed.

Thank you

RC1. As noted by the Editor, it would be extremely helpful to be able to view the Roldin manuscript describing PRAM. I must leave it to the editor's discretion whether publication of the present manuscript should be contingent on publication of Roldin et al (2019). References to Roldin (2018) should be corrected to Roldin (2019) throughout.

Reply. Thank you for the comment. We have now changed the reference Roldin (2018) → Roldin (2019) throughout the manuscript. We also have added a detailed description of the PRAM mechanism (L 98-112) and two references (Öström et al., 2017; Qi, 2018) which applied an earlier version of PRAM, though not using the acronym PRAM as the name came later. And as mentioned above the manuscript by Roldin et al., 2019 has been accepted for publication and PRAM from Roldin et al., 2019 can also be found at the following link https://doi.org/10.1594/PANGAEA.905102.

RC2. The discussion is pertinent and interesting but is also convoluted in places and difficult to read. It would benefit from a careful re-writing for language clarity and brevity. For example, lines 243-245 read: "Similarly, the current lack of peroxy radical autoxidation product mechanism for b-caryophyllene and isoprene result in Delta-Y=0 values for PRAM." How about saying something simpler, like: "Peroxy radical autoxidation reactions of b-caryophyllene and isoprene OH products are currently not included in PRAM, so the mechanisms are not compared in these cases (Fig 2b)."?

Reply. Thank you for bringing this to notice. We agree that parts of the manuscript will benefit from the use of simpler language for clarity. The line has now been omitted. We have rephrased the paragraph and the above line has been changed. Line omitted → ~~Similarly, the current lack of peroxy radical autoxidation product mechanism for β-caryophyllene and isoprene result in ΔY= 0 values for PRAM.~~

Line added (266-268) → Currently there are no experiments providing HOM yields from OH oxidation of β-caryophyllene, and hence, those species are not included in PRAM.

Line added (269-270) → Only MCM was used for modeling the mass yields for OH oxidation of isoprene due to current lack of PRAM mechanism for isoprene.

RC3. Comparisons with many published experimental results are cited in the text but are not included in the Tables (especially results where no PRAM is yet available). This reviewer suggests that it would be extremely helpful to move these simulation/data comparisons to the yield tables and figures (whether as points or as ranges). Then the agreement (or otherwise) could be summarized in the text without having to list all the specific numbers. This would make the text and its arguments easier to follow.

Reply. Thank you for the comment. I agree that moving the comparison between model to experiment values to the tables and figures can make it easier to follow arguments. Table 2 (a and b). and Table 3. have been updated to include comparison values between MCM+PRAM, MCM and experimental values for all compounds. Additionally Figures 1 and 2 have been replaced with four figures (Fig. 1, 2, 3 and 4). PRAM is currently not available for the ozonolyis of β-caryophyllene and β-pinene and for OH oxidation of β-caryophyllene and isoprene. Hence, we separated the figures to show how applying MCM+PRAM improves the mass yields estimation in comparison to only MCM compounds. Figure 1 and 3 show the improvement to mass yields by ozonolyis and OH, respectively for species where PRAM is available, whereas Figure 2. and 4. show the performance of MCM for oxidation of species not currently included in PRAM. Experimental values have also been added to the Figures 1,2 & 3 for better comparison. Changes to the text have been made at lines

L207-210→ The mass yields derived using MCM+PRAM for α-pinene ozonolysis are in good agreement with the experimental yields measured for similar mass loadings by Kristensen et al. (2017) and Pathak et al. (2007). The standalone MCM, on the other hand, severely under-predicts the mass yields for α-pinene ozonolysis.

L265-269→For β-caryophyllene, the modeled values are in good agreement with experimental measured yields in the range of mass loadings provided by Griffin (1999) and Tasoglou and Pandis (2015). Currently there are no experiments providing HOM yields from OH oxidation of β-caryophyllene, and hence, not included in PRAM

RC4. Perhaps I am missing something, but if the peroxy autoxidation reactions are not available for certain species/oxidant combinations, wouldn't it be more correct and less confusing to call the mechanism for those species/oxidant combinations MCM (or MCM-only) instead of MCM+PRAM or PRAM? (Throughout the manuscript, including Figure captions).

Reply. Thank you for pointing this out. You are right that it would be less confusing to refer to species/oxidant combination where no PRAM is available as MCM only. We have now corrected this throughout the manuscript.

RC5. Please explain whether some of the SOA formed in MCM is converted to different species in PRAM? Put another way, is the SOA formed in PRAM completely additional to that formed in MCM, or is there some conversion as a result of the autoxidation? If the latter, please discuss the level of "double-counting" of products in the MCM/PRAM side-by-side mass spectra figures.

Reply. Thank you for this comment. I assume you mean to ask if the compounds formed in PRAM are additional to compounds formed in MCM. Yes, the compounds formed in PRAM are additional to the compounds formed in MCM, ensuring that in the complete MCM+PRAM mechanism the total number of carbon atoms is conserved starting from the initial precursor. E.g. if you sum up the first generation RO_2 formed from α-pinene ozonolysis 91 % will react further in the MCM mechanism and the remaining 9 % will undergo autoxidation in PRAM. If only MCM chemistry is used in the model 100 % of the formed first generation RO_2 will continue in the MCM chemistry. Hence, when we implement PRAM together with MCM, the amount of MCM oxidation products are decreased. The most extreme case is limonene where 21.9 % of the first generation RO_2 go to PRAM and only 78.1 % follow the MCM chemistry (see Supplementary Table 1 in Roldin et al., 2019). An extract from Roldin et al., 2019:

"*When α-pinene is oxidized by O_3 one of the two ring structures is broken but a cyclobutyl ring is left intact in the RO_2 isomers ($C_{10}H_{15}O_4$) that are formed. According to quantum chemical calculations by Kurtén et al.,[20] the cyclobutyl ring inhibits multiple autoxidation steps and prevents the first intramolecular H-shifts reactions rates to exceed 0.3 s^{-1} at 298 K. In PRAM we therefore assigned a rate constants of 0.3 s^{-1} at 298 K for the first H-shift reaction (R11 in SI Table S4). Kurtén et al. also examined possible reaction pathways that can lead to opening of the cyclobutyl ring. According to Kurtén et al. the ring opening can likely occur via alkoxy radicals. Such pathways are also present in MCMv3.3.1 when the RO_2 isomer, with the MCM name C107O2, react with NO, NO_3 or other RO_2 and form an alkoxy radical C107O that can isomerize and react with O_2 and form a $C_{10}H_{15}O_5$ peroxy radical named C108O2. In PRAM we therefore included the possibility of such additional HOM formation pathway for α-pinene, which is initiated by the reaction between C107O2 and other RO_2 (R1152 followed by R20 and R12-R19 in SI Table S4).*"

RC6. The range of sensitivity conditions seems rather wide: the temperature extremes are beyond usual ambient temperatures. Please discuss whether the results from the extreme cases are likely to be environmentally or observationally relevant.

Reply. Thank you for this interesting comment. We have used 2 temperature extremes in the simulation of SOA mass yields, 258 K and 313 K respectively. Measurements have shown high concentrations of SOA in the free troposphere around 2-6.5 km (Heald et al., 2005). The lower temperature extreme of 258 K is a good

approximation for the free troposphere. Also, there have been a multitude of chamber experiments performed at these extreme temperatures (both at 258 and 313 K) (Kristensen et al., 2017; Saathoff and Naumann, 2009) and the aim of this study was to check the efficacy of MCM+PRAM in estimating yields at varying temperatures.

RC7. Given that SOA yields in an OFR are sensitive to particle surface area, several points arise. i) The Abstract states that MCM+PRAM overestimates OFR yields and gives increased particle surface area as the reason. The casual ("abstract-plus-figures") reader is left wondering why the simulations didn't use the same particle loadings as the literature. Is it possible to provide a little context in the abstract, to explain? ii)Does the over-prediction of modeled OFR SOA suggest that the literature experiments in the comparisons used too little seed to obtain stable yields? iii) The MCM+PRAM OFR overestimation is not readily apparent from Tables 2 and 3. It would be helpful to include lines that compare the results with measurements under the same loadings if possible, so the disagreement is more apparent to the reader.

Reply. Good question.

i) We have tested different particle surface area scenarios and subsequently chosen an area at which the yields estimation are not surface area limited (Supplement figure S1). On using low particle surface area we did not produce comparable particle mass loadings. Using the current particle surface area (corresponding to CS value of 0.067 s^{-1}) we are able to simulate mass loadings comparable with literature. We have now modified the comparison section where we compare the mass yields with similar particle loadings from literature. After re-examining the comparison of yields between experimental and simulations for similar particle loadings we find that for OH oxidation of α-pinene (Bruns et al., 2015) and β-pinene, mass yields are in good agreement with experimental values, whereas mass yields from OH oxidation of limonene are higher at similar particle loadings (Table 3). For ozonolysis, β-pinene mass yields are drastically under-predicted, while we see that α-pinene mass yields are in good agreement with results from Kang and Root (2007), after taking into account that the mass yields increase by a factor of 1.4 on adding seed particles. Changes to the abstract have now been made as follows:

→ Compared to experimental yields, the OFR simulations using MCM+PRAM yields were in good agreement for BVOCs oxidized by both O_3 and OH. On the other hand, a standalone MCM under-predicted the SOA mass yields.

ii) Yes. Ahlberg et al., (2019), Lambe et al., (2015) and Kang and Root (2007) have all found an increase in SOA mass yields when seed particles were used. The experiments by Friedman and Farmer (2018) have also

measured lower particle surface area leading to an underestimation of SOA yields. The extract from Friedman and Farmer (2018)

"*The SMPS utilized in our study detected a maximum particle diameter of 289 nm; this upper limit may lead to an underestimation of the total particle mass for particles growing to sizes larger than 289 nm and lower reported yields compared to other studies utilizing a larger particle size range*."

iii) The values to compare the simulation results with experiments have now been added to tables 2 and 3. Again we re-iterate that on re-examining the simulation and experimental values for similar particle loading we find that the mass yields generally agree well the experimental values (point (i)).

RC8. The earlier termination of the autoxidation mechanism in the OFR cases is attributed to "The higher absolute RO2 concentrations in the OFR simulations . . .. I.e. the high RO2 concentrations in the OFR cause termination of the peroxy radical autoxidation chain before the RO2 become highly oxygenated. . .." (line 229 ff.) This disagrees with the conclusions of Peng et al 2019 (https://doi.org/10.5194/acp-19-813-2019, 2019) who found that "for most types of RO2, their bimolecular fates in OFRs are mainly RO2+HO2 and RO2+NO, similar to chambers and atmospheric studies." At low NO, the high concentration of HO2 in the OFR leads to more rapid RO2 loss; at high NO, RO2+NO makes RO2 lifetime very short in the OFR. Please discuss whether the current modeling analysis is consistent with that work.

Reply. The study conducted by Peng et al., (2019) focuses on OH dominated atmospheres. The high concentrations of RO_2 described in the above sentence focuses on O_3 dominated atmosphere. Figure C1 shows that α-pinene – OH oxidation forms fewer dimers compared to ozonolysis. Figure C2 shows that our results are actually in agreement with the results from Peng et al., (2019). Compounds such as C10H18O5 (1.6), C10H18O6 (1.3), C10H18O7 (1.1), C10H18O8 (0.5) and C10H18O9 (0.2) are products of RO_2 + HO_2 reaction in PRAM (Roldin et al., 2019). The contribution of the above mentioned compounds are higher compared to the dimer contribution to SOA mass loadings in a OH dominated atmosphere, thereby supporting the argument that RO_2 + HO_2 reaction pathway dominates over RO_2 + RO_2 pathways in OH initiated and dominated atmospheres.

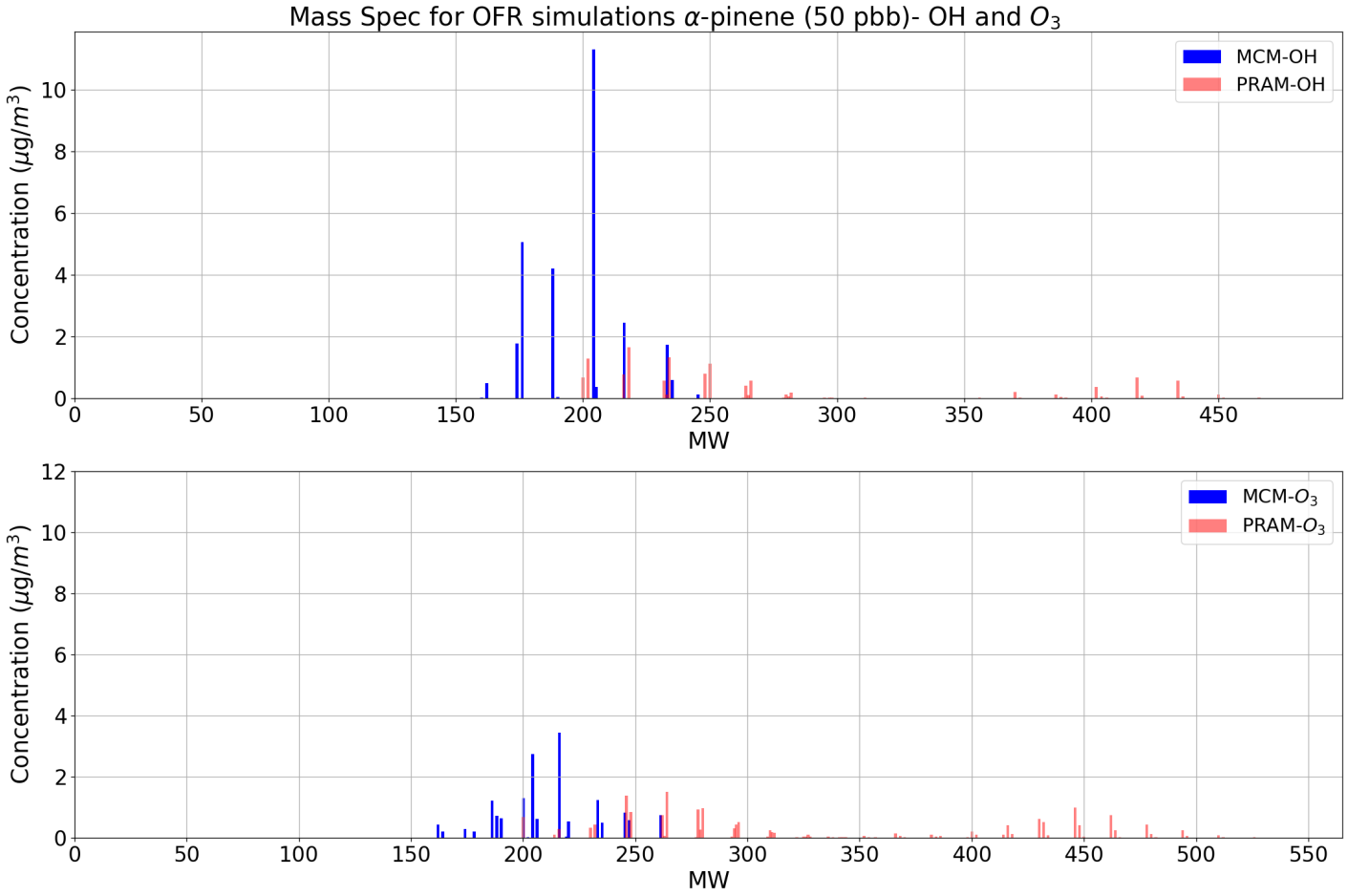

176 Figure C1. The upper panel shows the mass spectra for OFR simulations performed for α-pinene OH oxidation, while the lower
177 panel shows the mass spectra for α-pinene ozonolysis.

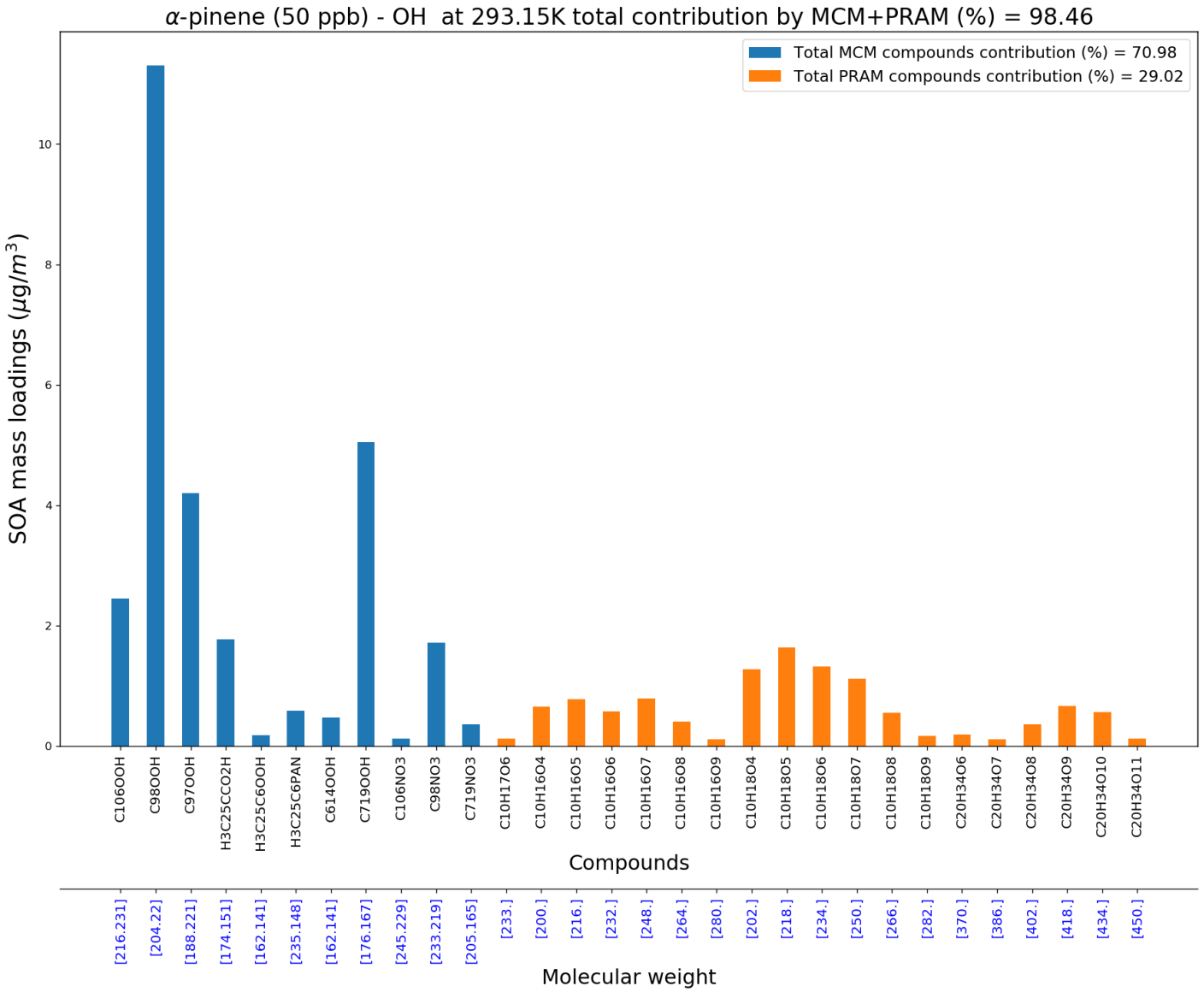

Figure C2. Compounds contributing to SOA mass loadings for α-pinene OH oxidation using an OFR setup.

Line 30: The scale of SOA contribution. . . is “still” subjected to high uncertainties. Is there a more recent reference than 2011?

Reply. Thank you for the comment. A new reference (Glasius and Goldstein, 2016) has been added.

Line 43: Does this mean Ehn (2014)? Ehn (2012) is not listed in the references.

Reply. Thank you for the comment. We have now added the new correct reference.

Ehn, M., Kleist, E., Junninen, H., Petäjä, T., Lönn, G., Schobesberger, S., Dal Maso, M., Trimborn, A., Kulmala, M., Worsnop, D. R., Wahner, A., Wildt, J. and Mentel, T. F.: Gas phase formation of extremely oxidized pinene reaction products in chamber and ambient air, Atmos. Chem. Phys., 12(11), 5113–5127, doi:10.5194/acp-12-5113-2012, 2012.

Line 58: Are there any measured O/C ratios in relevant systems that could be compared with?

Reply. Thank you for the comment. Yes Zhao et al., 2015 measured similar O/C ratios for both OH oxidation and ozonolysis of the monoterpenes with values ranging between 0.3-0.6. We have added this information in the manuscript as well.

Further they measured lower H/C ratio for SOA produced by monoterpene ozonolysis (experiments were carried out in dark with CO as OH scavenger), in comparison to OH oxidation of α-pinene and limonene, while O/C ratio were similar for both oxidation cases

Line 97: The timing seems confused: MCM+PRAM (Damian et al 2002) vs PRAM (Roldin et al 2018). Please clarify. (Did Damian et al really refer to MCM+PRAM?)

Reply. Thank you for the comment. I think I have made a typo by including MCM+PRAM here. It has now been removed.

Line 101: What sort of fraction of the peroxy radicals is considered in PRAM?

Reply. Thank you for the question. We have now added an explanation of the different fractions of peroxy radicals considered in PRAM. The section added is as follows:

Currently, in PRAM a maximum first generation RO_2 yield of 9% for α-pinene ozonolysis, 21.9 % for limonene ozonolysis, 2.5 % for α-pinene+OH, and 1% for both limonene+OH and β-pinene+OH first generation products are allowed to initiate autoxidation (Öström et al., 2017, Qi et al., 2018, Roldin et al., 2019).

Line 130-133: Please explain whether there is likely to be any bias from using two different systems to estimate p_0 for different species subsets?

Reply. We have not performed any studies aimed at trying to understand the bias resulting from using 2 different systems to estimate p_0. We use two different p_0 estimation methods as the information needed (eg. SMILES for PRAM) is not currently available to implement the same method to all compounds. Kurtén et al., (2016) have shown that Nannoolal method produces low estimates of saturation vapour pressure for multifunctional compounds due to the absence of hydro-peroxide or peroxy-acid group parameterizations. SIMPOL on the other hand, has shown to be in better agreement with pure-liquid vapour pressures of multifunctional compounds calculated using COSMO-RS (Conductor-like Screening Model for Real Solvents) (Eckert and Klamt, 2002; Kurtén et al., 2016).

Therefore, we have tried to use the most optimum way to utilize the current information to generate realistic p_0 values.

Line 188: I think the phrase “contribution to SOA mass” is misleading. It suggests proportion of the SOA made up by species “i”, whereas the figure actually shows “SOA mass yield”.

Reply. Yes I agree. I have now modified the text to:

→In Fig. 1 the upper panel A indicates the SOA mass yields derived on applying a coupled MCM+PRAM mechanism to ozonolysis of α-pinene and limonene (PRAM is only available for ozonolysis of α-pinene and limonene) and the lower panel B shows ratio of yields obtained by MCM and coupled MCM+PRAM.

Lines 217 & 221, and in general: When referring to “our model” It would be helpful to distinguish at that point which version is being used in each case (MCM+PRAM or MCM), so that the reader is reminded whether or not PRAM is being used. The distinction is made a few sentences later: a little reorganization would help this discussion.

Reply. In this context ‘our model’ refers to the MALTE-Box. We agree that its good to remind the reader about the case being used. Hence we have now specified the version being used for each comparison.

→Kang and Root (2007) measured a value of 0.2 for ozonolysis of α-pinene for an initial precursor VOC concentration of 100 ppbv, while we obtain ~0.25 (MCM+PRAM) for the similar initial precursor concentrations. The OFR yields for β-pinene (MCM-only) are significantly lower (0.02) than the values measured by Kang and Root (2007) wherein they measured a yield of 0.49 for similar initial precursor concentrations. Addition of seed particles promotes condensation, leading to increased SOA yields (Lambe et al., 2015) which was confirmed by Ahlberg et al, (2019).

Line 240: The values quoted in the text for OFR-simulation SOA yield from a-pinene ozonolysis do not match the values quoted in Table 2. Why the discrepancy?

Reply. The values in the text represented the yields for entire range of SOA mass loadings, whereas the tables only compared yields at corresponding loadings. It has now been changed to show values for corresponding simulated and experimental yields.

Line 270: This section needs an easier-to read introductory sentence.

Reply. This line has now been omitted. The introduction has been changed to:

→ The mass yields obtained by MCM+PRAM for α-pinene – OH oxidation are close to the measured values (Kristensen et al., 2017), while using only MCM under-predicts the mass yields (Figure 3, panel A and B, and Table 3).

Line 277 and following: Please list in Table 3 the experimental results of Kristensen 2017 and others cited in Section 3.2.

Reply. Done.

Line 273: It's not really true that Y=0 in these cases, since Y is the result of a comparison, and here there is nothing to compare (since there really isn't a "PRAM" for these species-oxidant combinations).

Reply. Yes true. We have omitted this line.

Line 289: It's usual to say that the model results are in good agreement with previous measurements, not the other way around.

Reply. Yes, it has been changed now.

→For β-caryophyllene, the modeled values are in good agreement with experimental measured yields in the range of mass loadings provided by Griffin (1999) and Tasoglou and Pandis (2015).

Line 274: Please briefly remind the reader why the simulations used more surface area than the experiments? It seems to be an important factor in the disagreement.

Reply. On re-examining, we have modified the conclusions. Changes have been made as follows:

→ Our yields for α-pinene agree well with the yields obtained by Bruns et al. (2015) where they measured yield of ~0.3 for mass loading of ~300 μg m^{-3} and equivalent OH exposures. Friedman and Farmer (2018) found mass yields of 0 - 0.086 for α-pinene (ammonium sulfate seeded experiment), 0- 0.12 for β-pinene (no seed particles) and 0-0.04 for limonene (no seed particles), by varying the OH exposures between 4.7 x 10^{10} – 7.4 x 10^{11} molecules cm^{-3} s. Our simulated yields for OH oxidation of α-pinene (~0.05 - 0.31), β-pinene (~ 0 - 0.1) and limonene suggest higher mass yields for α-pinene and limonene at equivalent mass loadings, while mass yields for β-pinene are in good agreement with the experimental yields. Friedman and Farmer (2018) suggest that the reason for this underestimation in mass yields could arise due to the exclusion of large particle sizes in the experiments and propose that these yields could represent lower bounds.

Line 302: This sentence is difficult to make sense of. Is this what is meant? "Varying NOx concentrations changes the fates of RO2 radicals formed during organic oxidation, thereby impacting . . ."

Reply. Yes your right. It has now been modified to:

Varying NO_x concentrations changes the fate of RO_2 radical formed during organic oxidations by altering HO_2/RO_2 ratio, thereby impacting the distribution of reaction products and aerosol formation (Presto et al., 2005; Zhao et al., 2018; Sarrafzadeh et al., 2016).

Line 368: Please be specific that the PRAM contribution increases with increasing NO for NO < 1ppb. (It's not quite clear the way it's currently written.)

Reply. Done.

Line 382: I suspect this means that the compounds shown in Fig 8 contribute >95% to the SOA mass loading when summed in decreasing order of contribution. Please clarify the text. (It's said better in the caption and in Line 385.)

Reply. Yes, these compounds contribute to >95% of SOA mass loadings regardless of the order of contribution. The text has been modified to:

Figure 10 shows the most important compounds from both the MCM and PRAM that together contribute to more than 95% of α-pinene ozonolysis SOA mass loading at 293.15 K.

Line 463: I think this means to say something like "We do not simulate appreciable mass yields from the oxidation of BVOCS with NO3". The current text claims to describe the behavior of the actual compounds, but I think it really intends to describe their behavior in the model. It's an important distinction.

Reply. Yes. The text has now been modified to:

The model does not simulate appreciable SOA mass yields for oxidation of BVOCs with NO_3, as PRAM currently does not consider autoxidation of RO_2 formed from NO_3 oxidation of VOCs.

Comments on the Figures:

1. Why are the points in the Figures arranged in clumps/streaks? Please explain early on.

Reply. The clumps are a result of SOA mass yields for the oxidation of specific oxidant concentration with varying BVOC concentration eg. 6 values of BVOC concentration (0 – 200 ppb) and specific oxidant concentration (5×10^{11} #/cm^3). This has now been explained in the figure captions (Fig 1).

→ The clumps are a result of SOA mass yields for the oxidation of specific oxidant concentration with varying BVOC concentration

2. The caption to Fig 1 says ". . . from simulations with MCM+PRAM and PRAM." Shouldn't it really say "MCM+PRAM and MCM"?

Reply. The lower panel actually shows $Y_{(MCM+PRAM)} - Y_{(MCM)}$ or effectively the contribution of PRAM.

3. Figs 1 & 2: Please denote the two panels 'a' and b' and refer to them that way in the caption and text. This would help the reader and might help clarify the flow of the discussion.

Reply. Done.

4. Figs 1 & 2: Please add notes to the figure captions to clarify which species are omitted from the comparison in each case (i.e. which species use MCM-only).

Reply. Done.

5. Figs 1 & 2, 2nd panels: It is sometimes hard to figure out whether MCM makes any contribution at all. Please make this clearer by either a) plotting the ratio $Y_{MCM} / Y_{(MCM+PRAM)}$ instead of (or in addition to) the difference between the two, or at least b) using the same gridline interval in both panels.

Reply. Good idea. The panel B of Figures 1 and 3 now show the ratio $Y_{MCM} / Y_{(MCM+PRAM)}$

6. Please mention Figure 3 somewhere in the text, or remove it.

Reply. Done. Figure 3 has now changed to Figure 5.

Figure 5. shows the yields derived from the oxidation of BVOCs by NO_3. Currently, as no PRAM is available for NO_3 oxidation, Figure 5 represents SOA yields derived using MCM.

Comments on the Tables:

1. Table 2: what are the figures in parentheses in the Experimental Yields column? Why are they not always present? Please explain.

Reply. The values in the parentheses represent the corresponding mass loadings for experimental yields. We have not added loadings for a few comparisons when the experimental loadings were similar to the simulated loadings. We have now included all experimental loadings in parantheses.

2. Table 2: Please include the b-pinene and b-caryophyllene MCM-to-literature comparisons mentioned in the text (lines 203-212).

Reply. Done.

3. Table S1a: To make this information easier to digest, I suggest listing the compounds in descending order of contribution to SOA mass. Also: Is this just the a-pinene ozonolysis case? Please clarify. If it's for various precursors, please indicate which precursor is relevant for each product.

Reply. Done. Yes these are compounds only for α-pinene ozonolysis case at different temperatures.

Minor Language Editing Suggestions:

Line 29: ". . . is still subject to . . ." (Not "subjected")

Reply. Done.

Line 134: "by contrast" might be a better phrase than "on the contrary"

Reply. Done.

Line 183 (suggestion): Move header for Section 3.1 to after "flow-tube experiments" (in line 187)

Reply. Good suggestion. Done.

Line 240: Replace "resulting" with "result".

Reply. This sentence has been omitted.

Line 243: the word "Similarly" seems strange here. (It would usually be understood to refer to the previous sentence). Perhaps this means: "As in the ozonolysis case"?

Reply. This sentence has been omitted.

Line 327-329: "Due to limited experimental constraints, PRAM presently does not consider autoxidation of RO2 formed from NO3 oxidation of VOCS". I suggest that moving this information to the top of the paragraph would help the reader more quickly make sense of the comparisons presented.

Reply. Done.

Line 340-342 almost duplicates Line 302. It would be good to combine these two sentences, for brevity.

Reply. Done.

Line 373: ". . . the formation OF more volatile . . ." (add word "of")

Reply. Done

Line 385: ". . . and decrease (no 's') to 0.27 at 293.15K AND to 0.1 at 313.15K" (add word "and")

Reply. Done

Line 389: Maybe this is "a weak dependence . . ..WHICH becomes more pronounced. . ."? ("which", not "but")

Reply. Done.

Line 419 duplicates some of lines 423-425. Please condense.

Reply. Done.

Line 467: (suggestion) "substantially lower than that of MCM"

Reply. Done.

Line 469: MCM *produces* more SVOCs, it doesn't just "contain" them.

Reply. Done

Line 481: delete word "respectively"

Reply. Done.

Line 477" "has paved THE way" (add word "the"). Or substitute something simpler like "helps us"

Reply. Done.

Reviewer 2

This is a good informative study that compares MCM and MCM+PRAM mechanisms to derive model capabilities of known peroxy radical autooxidation mechanisms.

Thank you

Following are some comments that are recommended to improve the current work:

RC1. Add a section on experimental details before model description. This could be just a summary of various experimental studies the work is using to evaluate the model with justifications for why they were chosen.

Reply. Done. The summary is now provided in the Supplementary material.

RC2. On page 17 the authors mention T-dependence of peroxy radical autotoxidation needs further improvement/validation. More details on their assumed T-dependence in PRAM are needed. For example, what was the assumed T-dependence as a function of precursor VOC, oxidant, NO etc.? What was the T-dependence of saturation vapor pressures of SVOCs in Figure 7? Seems there are 2 different T-dependence that need to be explicitly stated: (A) T-dependence of autooxidation chemistry (B) T-dependence of their C* i.e. saturation vapor pressure or a physical process of gas-particle partitioning. This is T-dependence is a very important part and needs to be discussed clearly. Also discuss measurements of such T-dependencies as applicable.

Reply. Yes they are 2 different temperature dependence that is addressed as follows:

(A).The temperature dependence in PRAM is based on quantum chemical calculations wherein the autoxidation rates correspond to an activation energy of 24 kcal/mol. The activation energies vary for autoxidation of different RO_2 from α-pinene ozonolysis between 22 and 29 kcal/mol (Rissanen et al., 2015), leading to varying autoxidation rates at different temperatures (Roldin et al., 2019).

(B). The functional group contribution methods SIMPOL and Nannoolal provide temperature dependent pure liquid saturation vapour pressures. Temperature is then used as an input parameter to the calculated p_0.

This information has now been added to the manuscript.

RC3 Figure 7: Would it be possible to start with a VBS fit at 313 K, and then derive the VBS fit at 258K or vice versa with these T-dependencies without having to run MCM+PRAM at each of these temperatures? This is important for regional and global models that rely on VBS and cannot run full MCM+PRAM.

Reply. This could be possible but not advisable as extending VBS for varying temperatures would lead to erroneous yield estimates. VBS does not change the total number of products for varying dependencies such as NO_x, RH or temperatures, but rather distributes volatility of products (Donahue et al., 2009). Our analysis of different compounds contributing to mass yields at different temperatures (Figure 10, S3 and S4, Table S1-

S3) show that different products contribute to mass yields at differing temperatures. Using a VBS hence for estimating the yields derived for 258 K and extending it to 313K would result in misleading SOA mass yields.

RC4 Do the authors have any recommendations for condensed versions of MCM+PRAM that could be used in regional and global models to predict SOA yields and their oxidation state?

Reply. Yes. A condensed version of PRAM to be applied in regional and global models has been tested by reducing the number of reactions and species by lumping them into 2 sets of dimers specifically 1.representing HOM formed by ozonolysis of monoterpenes and 2. HOM formed by OH oxidation (Roldin et al., 2019). Furthermore, the author cautions that full PRAM be evaluated for conditions where a major part of RO_2 pool originates from precursors that do not contribute substantially to HOM formation, such as environments with high isoprene concentrations, before being applied to global and regional models (Roldin et al., 2019). More details can be found in Roldin et al., (2019). We have made this addition to the conclusions sections:

→ Furthermore, implementation of a condensed PRAM version to regional and global models has been tested but still need further validation (Roldin et al., 2019).

References

Bruns, E. A., El Haddad, I., Keller, A., Klein, F., Kumar, N. K., Pieber, S. M., Corbin, J. C., Slowik, J. G., Brune, W. H., Baltensperger, U. and Prévôt, A. S. H.: Inter-comparison of laboratory smog chamber and flow reactor systems on organic aerosol yield and composition, Atmos. Meas. Tech., 8(6), 2315–2332, doi:10.5194/amt-8-2315-2015, 2015.

Donahue, N. M., Robinson, A. L. and Pandis, S. N.: Atmospheric organic particulate matter: From smoke to secondary organic aerosol, Atmos. Environ., 43(1), 94–106, doi:https://doi.org/10.1016/j.atmosenv.2008.09.055, 2009.

Eckert, F. and Klamt, A.: Fast Solvent Screening via Quantum Chemistry: COSMO-RS Approach, AIChE J., 48(2), 369–385, doi:10.1002/aic.690480220, 2002.

Friedman, B. and Farmer, D. K.: SOA and gas phase organic acid yields from the sequential photooxidation of seven monoterpenes, Atmos. Environ., 187(January), 335–345, doi:10.1016/j.atmosenv.2018.06.003, 2018.

Glasius, M. and Goldstein, A. H.: Recent Discoveries and Future Challenges in Atmospheric Organic Chemistry, Environ. Sci. Technol., 50(6), 2754–2764, doi:10.1021/acs.est.5b05105, 2016.

Heald, C. L., Jacob, D. J., Park, R. J., Russell, L. M., Huebert, B. J., Seinfeld, J. H., Liao, H. and Weber, R. J.: A large organic aerosol source in the free troposphere missing from current models, Geophys. Res. Lett., 32(18), 1–4, doi:10.1029/2005GL023831, 2005.

Kang, E. and Root, M. J.: Introducing the concept of Potential Aerosol Mass (PAM), Atmos. Chem. Phys., (7), 5727–5744 [online] Available from: www.atmos-chem-phys.net/6/3131/2006/%5Cnhttp://link.springer.-com/10.1007/978-3-642-34216-5%5Cnwww.atmos-chem-phys.net/15/253/2015/%5Cnhttp://www.atmos-chem-phys.net/15/253/2015/%5Cnhttp://www.sciencemag.org/content/331/6022/1295.abstract%5Cnhttp://www.tan, 2007.

Kristensen, K., Jensen, L. N., Glasius, M. and Bilde, M.: The effect of sub-zero temperature on the formation and composition of secondary organic aerosol from ozonolysis of alpha-pinene, Environ. Sci. Process. Impacts, 19(10), 1220–1234, doi:10.1039/c7em00231a, 2017.

Kurtén, T., Tiusanen, K., Roldin, P., Rissanen, M., Luy, J. N., Boy, M., Ehn, M. and Donahue, N.: α-Pinene Autoxidation Products May Not Have Extremely Low Saturation Vapor Pressures Despite High O:C Ratios, J. Phys. Chem. A, 120(16), 2569–2582, doi:10.1021/acs.jpca.6b02196, 2016.

Lambe, A. T., Chhabra, P. S., Onasch, T. B., Brune, W. H., Hunter, J. F., Kroll, J. H., Cummings, M. J., Brogan, J. F., Parmar, Y., Worsnop, D. R., Kolb, C. E. and Davidovits, P.: Effect of oxidant concentration, exposure time, and seed particles on secondary organic aerosol chemical composition and yield, Atmos. Chem. Phys., 15(6), 3063–3075, doi:10.5194/acp-15-3063-2015, 2015.

Öström, E., Putian, Z., Schurgers, G., Mishurov, M., Kivekäs, N. and Lihavainen, H.: Modeling the role of highly oxidized multifunctional organic molecules for the growth of new particles over the boreal forest region, , 8887–8901, 2017.

Peng, Z., Lee-Taylor, J., Orlando, J. J., Tyndall, G. S. and Jimenez, J. L.: Organic peroxy radical chemistry in oxidation flow reactors and environmental chambers and their atmospheric relevance, Atmos. Chem. Phys., 19(2), 813–834, doi:10.5194/acp-19-813-2019, 2019.

Qi, X.: Modelling studies of HOMs and their contributions to new particle for-mation and growth: comparison of boreal forest in Finland and a polluted environment in China, Suppl. Atmos. Chem. Phys, 18, 11779–11791, doi:10.5194/acp-18-11779-2018-supplement, 2018.

Rissanen, M. P., Kurtén, T., Sipilä, M., Thornton, J. A., Kausiala, O., Garmash, O., Kjaergaard, H. G., Petäjä, T., Worsnop, D. R., Ehn, M. and Kulmala, M.: Effects of chemical complexity on the autoxidation mechanisms of endocyclic alkene ozonolysis products: From methylcyclohexenes toward understanding α-pinene, J. Phys. Chem. A, 119(19), 4633–4650, doi:10.1021/jp510966g, 2015.

Saathoff, H. and Naumann, K.-H.: Temperature dependence of yields of secondary organic aerosols from the ozonolysis of α-pinene and limonene, Atmos. Chem. Phys., (March), 4–15, doi:10.5194/acp-9-1551-2009, 2009.

Zhao, D. F., Kaminski, M., Schlag, P., Fuchs, H., Acir, I. H., Bohn, B., Häseler, R., Kiendler-Scharr, A., Rohrer, F., Tillmann, R., Wang, M. J., Wegener, R., Wildt, J., Wahner, A. and Mentel, T. F.: Secondary or-

ganic aerosol formation from hydroxyl radical oxidation and ozonolysis of monoterpenes, Atmos. Chem. Phys., 15(2), 991–1012, doi:10.5194/acp-15-991-2015, 2015.

Aerosol Mass yields of selected Biogenic Volatile Organic Compounds – a theoretical study with near explicit gas-phase chemistry

Carlton Xavier[1], Anton Rusanen[1], Putian Zhou[1], Chen Dean[1], Lukas Pichelstofer[1], Pontus Roldin[2], Michael Boy[1]

[1]Institute for Atmospheric and Earth Systems Research (INAR), Physics, University of Helsinki

[2]Division of Nuclear Physics, Lund University, Box 118, SE-22100, Lund, Sweden

Correspondence : Carlton Xavier (carlton.xavier@helsinki.fi), Michael Boy (michael.boy@helsinki.fi)

Abstract

In this study we modeled secondary organic aerosols (SOA) mass loadings from the oxidation (by O_3, OH and NO_3) of five representative Biogenic Volatile Organic compounds (BVOCs): isoprene, endocyclic bond containing monoterpenes (α-pinene and limonene), exocyclic double bond compound (β-pinene) and a sesquiterpene (β-caryophyllene). The simulations were designed to replicate idealized smog chamber and oxidative flow reactors (OFR). The master chemical mechanism (MCM) together with the peroxy radical autoxidation mechanism (PRAM), were used to simulate the gas-phase chemistry. The aim of this study was to compare the potency of MCM and MCM+PRAM in predicting SOA formation. SOA yields were in good agreement with experimental values for chamber simulations when MCM+PRAM was applied, while a standalone MCM under-predicted the SOA yields. Compared to experimental yields, the OFR simulations using MCM+PRAM yields were in good agreement for BVOCs oxidized by both O_3 and OH. On the other hand, a standalone MCM under-predicted the SOA mass yields. SOA yields increased with decreasing temperatures and NO concentrations and vice-versa. This highlights the limitations posed when using fixed SOA yields in a majority of global and regional models. Few compounds that play a crucial role (>95% of mass load) in contributing to SOA mass increase (using MCM+PRAM) are identified. The results further emphasized that incorporating PRAM in conjunction with MCM does improve SOA mass yields estimation.

1. Introduction

Atmospheric secondary organic aerosols, formed from gas to particle phase conversion of the oxidation products of volatile organic compounds (VOC) significantly impact the organic aerosol mass loadings (Griffin, 1999; Kanakidou et al., 2005). However, the scale of SOA contribution to the aerosol particle mass is still subject to high uncertainties (Hao et al., 2011,Glasius and Goldstein, 2016). The elevated

aerosol particle concentrations are shown to have inimical effects on health (Miller et al., 2007), and a varying degree of influence on the climate by forming cloud condensation nuclei (CCN), altering the cloud properties and radiative balance (Rosenfeld et al., 2014; Schmale et al., 2018). Therefore, it is acutely necessary to understand the role and contributions of SOA to the particle loading in the atmosphere. Biogenic VOCs from forest are estimated to contribute to about 90% of VOCs emissions globally (Guenther et al., 1995, 1999 and 2000). The most important BVOCs for SOA formation are isoprene (C_5H_8), monoterpenes ($C_{10}H_{16}$) and sesquiterpenes ($C_{15}H_{24}$). These compounds are all alkenes containing at least one carbon-carbon double bond, enabling them to undergo oxidation by the dominant atmospheric oxidants: the hydroxyl radical (OH), ozone (O_3) and the nitrate radical (NO_3). For some of the terpenes, initial oxidation steps can lead to formation of highly oxygenated organic molecules (HOM). These HOMs generally have low volatilities and can condense nearly irreversibly, thereby producing SOA (Ehn et al., 2014). HOMs, detected in both the ambient atmosphere and chamber experiments (Ehn et al., 2012) are formed by autoxidation (Berndt et al., 2016; Crounse and Nielsen, 2013) wherein peroxy radicals (RO_2) undergo subsequent intramolecular H-shifts accompanied by rapid reactions with O_2. Autoxidation hence results in compounds containing multiple functional groups such as hydroxyls, peroxides and carbonyls (Bianchi et al., 2017,Bianchi et al., 2019).

A majority of chamber and flow-tube experiments have focused on HOM formation from the oxidation of various VOCs and their contribution to SOA mass loadings (Ehn et al., 2014; Kristensen et al., 2017). Oxidation of isoprene (Liu et al., 2016), endocyclic monoterpenes containing reactive double bonds such as α-pinene and limonene (Zhao et al., 2015) , or exocyclic double bond containing compounds such as β-pinene (Jokinen et al., 2015) and sesquiterpenes such as β-caryophyllene (Chen et al., 2012) have been investigated. The SOA forming potential of various BVOCs depends on the isomeric structures (Friedman and Farmer, 2018; Keywood et al., 2004). Ozonolysis of compounds containing reactive endocyclic bonds such as α-pinene produce higher SOA mass yields of 41% in comparison to those with exocyclic bonds (β-pinene), which produce mass yields of 17 % (Lee et al., 2006a). One explanation for this dependence on the isomeric structure is attributed to the formation of HOMs (Ehn et al., 2014). Another important factor influencing HOM formation is the initial oxidant, as pointed out by Zhao and co-workers (2015). They showed that the SOA formation by OH oxidation of α-pinene and limonene were lower when compared to their SOA formed by ozonolysis. Further they measured lower H/C ratio for SOA produced by monoterpene ozonolysis (experiments were carried out in dark with CO as OH scavenger), in comparison to OH oxidation of α-pinene and limonene, while O/C ratio were similar for both oxidation cases. This was attributed to the formation of RO_2 radicals (monoterpenes $+O_3$) which undergo internal hydrogen shifts and subsequently react with another RO_2 radical, to form compounds containing carbonyl groups while losing hydrogen atoms in the

process. A similar analysis was conducted by Draper et al. (2015), who showed that an increase in NO_2 concentration reduced α-pinene ozonolysis SOA mass yields, while no appreciable reduction in mass yields are reported for β-pinene and Δ^3- carene ozonolysis. On the other hand, the mass yields from limonene ozonolysis increased with increasing NO_2 concentrations (Draper et al., 2015). This disparity in mass yields for different BVOCs in the presence of NO_2 is possibly caused by the formation of high MW oligomers (or lack of in case of α-pinene) through oxidation with NO_3 that contribute to SOA mass loadings (Draper et al., 2015).

Due to computational limitations, many regional and canopy scale atmospheric chemistry models generally use isoprene and/or a representative monoterpene (generally α-pinene), to model SOA yields (Friedman and Farmer, 2018). The SOA yields of different monoterpenes vary with structure, NO_x and temperature (Friedman and Farmer, 2018; Kristensen et al., 2017; Presto et al., 2005). This poses a limitation on using representative monoterpene fixed SOA yields in many of the global models and increases uncertainties in predicting cloud condensation nuclei concentrations, cloud droplet number concentrations and radiative balance due to aerosol loading's.

This work aims to investigate the SOA mass loading from the oxidation products of BVOCs with the atmospheric oxidants OH, O_3 and NO_3 with a specific focus on the BVOCs isoprene, α-pinene, β-pinene, limonene and β-caryophyllene. Further we study the effect of varying temperature (258.15 K – 313.15 K) and NO concentrations (0 - 5 ppb) on α-pinene oxidation mass yields. We use the master chemical mechanism (MCMv3.3.1) (Jenkin et al., 1997, 2012 and 2015; Saunders et al., 2003), a near explicit gas-phase chemical mechanism together with peroxy radical autoxidation mechanism (PRAM, Roldin et al., 2019) (PRAM + MCM). The aim is to understand the importance and contribution of peroxy radical autoxidation products to the SOA mass yields from terpenes.

2. **Model description**

2.1 **Malte Box**

MALTE (Model to predict new Aerosol formation in Lower TropospherE) is a one-dimensional model consisting of modules calculating boundary layer meteorology, emissions of BVOCs, gas-phase chemistry and aerosol dynamics with the aim to simulate particle distribution and growth in the lower troposphere (Boy et al., 2006). In this study, a zero-dimensional version, MALTE-Box is applied to simulate an ideal chamber and flow-tube environment (i.e. no wall losses effects are considered in this study). For the

simulations performed in this study the emission module was switched off while only employing the gas-phase chemistry and aerosol dynamics module.

Kinetic preprocessor (KPP) is used to generate a system of coupled differential equations to solve the gas-phase chemistry schemes (Damian et al., 2002). The peroxy radical autoxidation mechanism (PRAM), (Roldin et al., 2019, Qi et al., 2018, Öström et al., 2017), formulated based on the oxidation of monoterpenes as described by Ehn et al. (2014) was incorporated alongside MCMv3.3.1. PRAM explicitly describes the formation and evolution of peroxy radicals (RO_2) from the ozonolysis and OH oxidation of monoterpenes, driven by subsequent H-shifts and O_2 additions. The current version of PRAM based on experimental and theoretical studies, considers HOM autoxidation for a fraction of the peroxy radicals formed during the ozonolysis of α-pinene and limonene and OH oxidation of α-pinene, β-pinene and limonene. This is achieved by assigning species specific molar yields for the formation of first RO_2, which subsequently initiates the autoxidation chain (Roldin et al., 2019). Currently, in PRAM a maximum first generation RO_2 yield of 9% for α-pinene ozonolysis, 21.9 % for limonene ozonolysis, 2.5 % for α-pinene+OH, and 1% for both limonene+OH and β-pinene+OH first generation products are allowed to initiate autoxidation (Roldin et al., 2019). For β-pinene ozonolysis the molar yield of RO_2 is minor (<0.1 %) (Roldin et al., 2019, Ehn et al. 2014) and hence not considered in this work. The above mentioned RO_2 molar yields used in this work are close to the experimental values obtained in both smog chamber and flow tube experiments. Ehn et al. (2014) measured an RO_2 yield of ~7% for α-pinene ozonolysis and ~17% for limonene ozonolysis, whereas Jokinen et al. (2015) measured 0.58 % and 0.93 % for OH oxidation of β-pinene and limonene respectively. The autoxidation is terminated by bimolecular reactions, wherein the RO_2 formed reacts with NO, HO_2 or other peroxy radicals, thereby forming alkoxy radicals, closed shell monomers or dimers (Roldin et al., 2019). The PRAM considers temperature dependent autoxidation reaction rates, which is important when investigating the SOA mass yields at varying temperatures (Table 1c). The temperature dependence in PRAM is based on quantum chemical calculations wherein the autoxidation rates correspond to an activation energy of 24 kcal/mol. The activation energies vary for autoxidation of different RO_2 from α-pinene ozonolysis between 22 and 29 kcal/mol (Rissanen et al., 2015), leading to varying autoxidation rates at different temperatures (Roldin et al., 2019). It should be noted that the temperature dependence in PRAM is a first of its kind but needs further evaluation using recent measurements of HOM formation at different temperatures (e.g. Quéléver et al.2018).

The aerosol dynamics are simulated using the University of Helsinki Multicomponent Aerosol model (UHMA) originally from Korhonen et al. (2004). The model has undergone significant development since then to allow simulation with all the compounds from MCM. It now supports an unlimited number of

condensing vapors and solves condensation using the analytical predictor of condensation method from Jacobson (1997). The condensation algorithm considers both, the Kelvin effect and Raoult's law. The processes included in the model are nucleation, condensation, evaporation, coagulation and deposition. The discretization of the size distribution and the time evolution is modeled with the moving section approach, with optional redistribution to a fixed grid. In this work, the redistribution is active to make the coagulation more accurate, since it requires that grid points are available near the size of the coagulated particles. In this study nucleation and deposition are not active, and hence are not considered. A total of 100 size bins ranging from 1nm to 20µm with the fixed grid was applied for this study.

A group contribution method based on Nannoolal et al. (2008) using the UManSysProp online system (Topping, 2016) was used to estimate the pure liquid saturation vapor pressures (p_0) of the organic compounds in MCMv3.3.1. For the PRAM species, p_0 were estimated using the functional group method SIMPOL (Pankow and Asher, 2008; see Roldin et al., 2019 for details). Temperature was used as an input to estimate p_0 for both the group contribution methods.

2.2 **Simulations**

The simulations performed in this study are aimed to closely resemble an idealized smog chamber (batch mode setup) and an Oxidative Flow Reactor (OFR) without interactions between the gas phase and the system walls. For the chamber runs, the VOC and oxidants were introduced at the beginning (time, t=0 sec), set to certain concentrations and then allowed to react. Both chamber and OFR simulations are performed using ammonium sulfate seed particles which are introduced at time t=0. The condensation sink (CS) was inferred from the size distribution of seed particles used in the model. The CS for the chamber and OFR simulations was set to 0.00067 s^{-1} and 0.067 s^{-1} respectively. SOA mass yields obtained using an OFR are sensitive to short residence time used, hence the seed particle surface area should be chosen in order to overcome the mass yield underestimation (Ahlberg et al., 2019). CS sensitivity runs (Supplement Figure S1) were performed for α-pinene-O_3 to determine the CS for which there are no appreciable change in mass yields with increasing particle surface.

The simulation for the chamber setup is run for a maximum time of 24 hours and ends when either of the 2 criteria are satisfied: (1) the simulation time reaches the 24-hour mark or (2) 90 % of the initial precursor VOC has reacted away. In the latter case the simulation is continued for an additional 2 hours to ensure enough time for the vapors to condense onto the seed particles. By contrast, the OFR runs were simulated for a maximum residence time of 100 seconds, ensuring all initial precursor vapors were oxidized. Seed particles were also added in the OFR simulations. The oxidant concentrations used for the OFR

simulations are significantly higher in comparison to the simulated chamber runs (~2 orders of magnitude larger). The time step for the chamber and flow-tube simulations are set to t=10 s and t =0.1 s respectively. The runs performed were oxidant specific (i.e. VOCs would be oxidized by only one specific oxidant at any given time). For the O_3 specific simulations no OH could form in both, OFR and chamber setups, thus enabling oxidation of O_3 to be the only pathway.

The simulations were performed at atmospheric relevant NO_x (NO_x = NO +NO_2) concentrations, corresponding to [NO]=0.5 ppb and [NO_2] = 2.0 ppb conditions with the relative humidity (RH) set to 60 % and temperature to 293.15 K. The RH value considered in this study is based on previous published experimental studies performed at ~60 % in both smog chamber (Bruns et al., 2015a; Ehn et al., 2014; Stirnweis et al., 2017) and OFR (Ahlberg et al. et al., 2018). α-pinene ozonolysis runs were performed at four different temperatures: 258.15 K, 278.15 K, 303.15K and 313.15 K, respectively. SOA mass yields are expected to increase with decreasing temperature (Saathoff and Naumann, 2009). A similar temperature dependence was observed by Kristensen et al. (2017) who observed SOA mass yield from α-pinene ozonolysis at ~ 40 % and ~20 % at 258 K and 293 K respectively. Analogous to analyzing the effect of varying temperature on SOA yields, we study the variation in α-pinene ozonolysis SOA mass yields by varying the NO_x concentrations. SOA yields for α-pinene ozonolysis at high NO_x conditions should be suppressed (Ng and Chhabra, 2007), which could be due to the production of relatively, volatile organic nitrates under high NO_x conditions as compared to less volatile products during low NO_x conditions (Presto et al., 2005).

Furthermore, two different chemistry schemes were applied for the simulations. One scheme consisted of only the MCM chemistry mechanism and the second included the MCM+PRAM chemistry mechanism. Table 1a shows the concentrations of different BVOCs and Table 1b shows the oxidants concentrations used for the simulations.

Table 1a. Concentrations of different BVOCs

α-pinene (ppb)	**β-pinene (ppb)**	**Isoprene (ppb)**	**Limonene (ppb)**	**β-caryophyllene (ppb)**
0.5, 1.0, 5.0, 50.0, 100.0, 200.0	0.5, 1.0, 5.0, 50.0, 100.0, 200.0	5.0, 50.0, 100.0, 200.0	1.0, 5.0, 50.0, 100.0, 200.0	0.5, 1.0, 2.0, 5.0, 10.0

665 **Table 1b**. Concentrations of different oxidants for chamber and flow-tube runs

OH (* 10^6 #/cm^3) - chamber **OH (* 10^8 #/cm^3) - OFR**	**O_3 (* 10^{11} #/cm^3) - chamber** **O_3 (* 10^{13} #/cm^3) - OFR**	**NO_3 (* 10^7 #/cm^3) - chamber** **NO_3 (* 10^9 #/cm^3) - OFR**
2.0, 5.0 ,10.0, 50.0,100.0	1.0, 5.0 ,10.0, 50.0,100.0	1.0, 5.0 ,10.0, 50.0,100.0

666

667 **Table 1c**. NO concentrations and temperatures used for α-pinene ozonolysis

NO (ppb)	0.5 (default), 0, 0.2, 1, 2, 5
Temperature (K)	293.15 (default), 258.15, 278.15, 303.15, 313.15

668

669 **2.3 Mass Yields**

670 The SOA mass yields (Y) are determined by calculating the ratio of the amount of SOA or mass
671 concentration of organic aerosol formed (C_{OA}) to the amount of VOC (ΔVOC) reacted:

672 $$Y = \frac{C_{OA}}{\Delta VOC} \qquad (1)$$

673 A volatility basis set is fit to the data to obtain the volatility distribution. In this study equilibrium
674 partitioning was only assumed for deriving the volatility distribution based on the model simulations.
675 Following Donahue et al. (2006), the SOA is assumed to be in equilibrium with the gas-phase and using the
676 effective saturation concentration C_i^* spaced logarithmically. The individual product partitioning to the
677 particle phase can be estimated using

678 $$E_i = \left(1 + \frac{C_i^*}{C_{OA}}\right)^{-1} \qquad (2)$$

679 Where E_i is the fraction of species in the condensed particle phase. The above equation determines the
680 fraction of species in the particle phase as well as in the gas phase. For example, if we assume C_{OA} =10 μg m^{-3}
681 a species with C^* = 10 μg m^{-3} will partition 50 % to condensed phase and the rest 50% will reside in the gas
682 phase. The fidelity of this equilibrium partitioning enables the parameterization of product vapors in volatility
683 C^* bins that are near the C_{OA} concentrations (Henry et al., 2012).

684

3. Results and Discussion

SOA mass yields were simulated for the oxidation of various biogenic volatile organic compounds (isoprene, α-pinene, limonene and β-caryophyllene, β-pinene) by dominant atmospheric oxidants OH, O_3 and NO_3. The following section examines the comparison between the yields derived using MCM+PRAM and a standalone MCM for chamber and flow-tube experiments.

3.1 BVOCs – O_3 chamber and flow-tube simulations

In Fig. 1 panel A indicates the SOA mass yields derived on applying a coupled MCM+PRAM mechanism to ozonolysis of α-pinene and limonene (PRAM is only available for ozonolysis of α-pinene and limonene) and the lower panel B shows ratio of yields obtained by MCM and coupled MCM+PRAM.

The abscissa, depicted on a log scale, considers the entire range of SOA mass loadings from 1-1150 $\mu g/m^{-3}$. Each data point is representative of simulated SOA mass yields resulting from variable BVOC loading. The resulting mass yields for α-pinene in the range shown in Table 2a. are consistent with the yields found in various smog chamber experiments.The mass yields derived using MCM+PRAM for α-pinene ozonolysis are in good agreement with the experimental yields measured for similar mass loadings by Kristensen et al. (2017) and Pathak et al. (2007). The standalone MCM, on the other hand, severely under-predicts the mass yields for α-pinene ozonolysis. The MCM+PRAM also shows better agreement with experiments when estimating the lower range mass yields for SOA mass loadings of < 15 $\mu g\ m^{-3}$. This is supported by the values obtained by Shilling et al. (2008), where the authors measured a 0.09 yield from α-pinene ozonolysis for SOA mass loading of 10.6 $\mu g\ m^{-3}$. Limonene ozonolysis mass yields using MCM+PRAM in comparison to standalone MCM, are much closer to the values given by Waring (2016).

The formation of HOM from β-pinene ozonolysis is low (Ehn et al., 2014; Jokinen et al., 2015) and hence not considered in PRAM. The peroxy radical autoxidation mechanism for β-caryophyllene ozonolysis has not yet been developed and therefore, not considered in PRAM. When comparing the measured mass yield values for β-caryophyllene (Chen et al. 2012) and β-pinene ozonolysis (Griffin (1999) and Pathak et al. (2008)) to the modeled values using the MCM scheme, it is evident that the MCM scheme drastically under-predicts the SOA mass yields (Fig. 2).

Today oxidation flow reactor (OFR) experiments are complementing the traditional batch mode smog chamber experiments. The OFR generally exhibits lower mass yields compared to the smog chamber experiments at ranges of equivalent oxidant exposure (Lambe et al., 2015). We modeled flow-tube simulation

after the potential aerosol mass (PAM) OFR, where the residence time is in the order of a few to several minutes (Lambe et al., 2011). The model simulations are performed with a maximum residence time of 100 seconds with O_3 exposures ranging from 1.0 x 10^{15} – 1.0 x 10^{17} molecules cm^{-3} s (residence time x [O_3]). Kang and Root (2007) measured a value of 0.2 for ozonolysis of α-pinene for an initial precursor VOC concentration of 100 ppbv, while we obtain ~0.25 (MCM+PRAM) for the similar initial precursor concentrations. The OFR yields for β-pinene (MCM-only) are significantly lower (0.02) than the values measured by Kang and Root (2007) wherein they measured a yield of 0.49 for similar initial precursor concentrations. Addition of seed particles promotes condensation, leading to increased SOA yields (Lambe et al., 2015) which was confirmed by Ahlberg et al, (2019). Kang and Root (2007) found that using seed particles, the yield from α-pinene ozonolysis increased by a factor of ~1.4 which can explain our yields for α-pinene ozonolysis simulations. The mass spectra plot (Figure S2) shows that PRAM contributes the majority of dimers to the particle phase, while MCM dominate monomer contribution. Another interesting facet of Figure S2 are the different condensing compounds in both OFR and chamber simulations. The higher absolute RO_2 concentrations in the OFR simulations explain the lower concentration of HOM monomers and dimers relative to the chamber simulations, i.e. the high RO_2 concentrations in the OFR cause termination of the peroxy radical autoxidation chain before the RO_2 become highly oxygenated, thereby influencing SOA yields. Hence, this should be taken into account when using yields from OFR as inputs to regional and global models.

Table 2a. Mass yields for BVOCs ozonolysis at 293 K for different range of mass loadings using a chamber[†] setup. The values in parenthesis in the column Experimental yields indicates the corresponding experimental mass loadings.

SOA mass loading (µg m^{-3})	**MCM + PRAM mass yields range**	**MCM mass yields range**	**BVOC**	**Experimental yields**	**References**
0– 15[†]	0.07– 0 .08	0.00 – 0.06	α-pinene	0.09 (10.6)	Shilling et al. (2008)
16 - 60[†]	0.12 – 0.20	0.06 – 0.11	α-pinene	0.16 – 0.21 (15 -60)	Pathak et al. (2007)
61 – 200[†]	0.22 – 0.30	0.12 – 0.15	α-pinene	0.22 (62)	Kristensen et al. (2017)
1.1– 550[†]	0.24 -0.48	0.007-0.06	limonene	0.26 (1.7)	Waring (2016)

0 - 100[†]	0 – 0.09[‼]	0 – 0.09	β-pinene	0.03-0.22 (7.2 - 100)	Griffin (1999)
0 -10[†]	0 – 0.01[‼]	0 – 0.01	β-caryophyllene	0.13 (1.8)	Chen et al. (2012)

733 [‼]indicates that no PRAM mechanism available yet i.e the yields are same as the MCM yields.

Table 2b. Mass yields for BVOCs ozonolysis at 293 K for different range of mass loadings using an OFR[‖] setup.

SOA mass loading (ppb)	**MCM + PRAM mass yields range**	**MCM mass yields range**	**BVOC**	**Experimental yields**	**References**
0-100[‖]	0.07-0.25	0-0.13	α-pinene	0.2 (100)	Kang and Root (2007)
0-156[‖]	0 – 0.02[‼]	0 – 0.02	β-pinene	0.49 (156)	Kang and Root (2007)

734 "indicates that no PRAM mechanism available yet i.e the yields are same as the MCM yields.

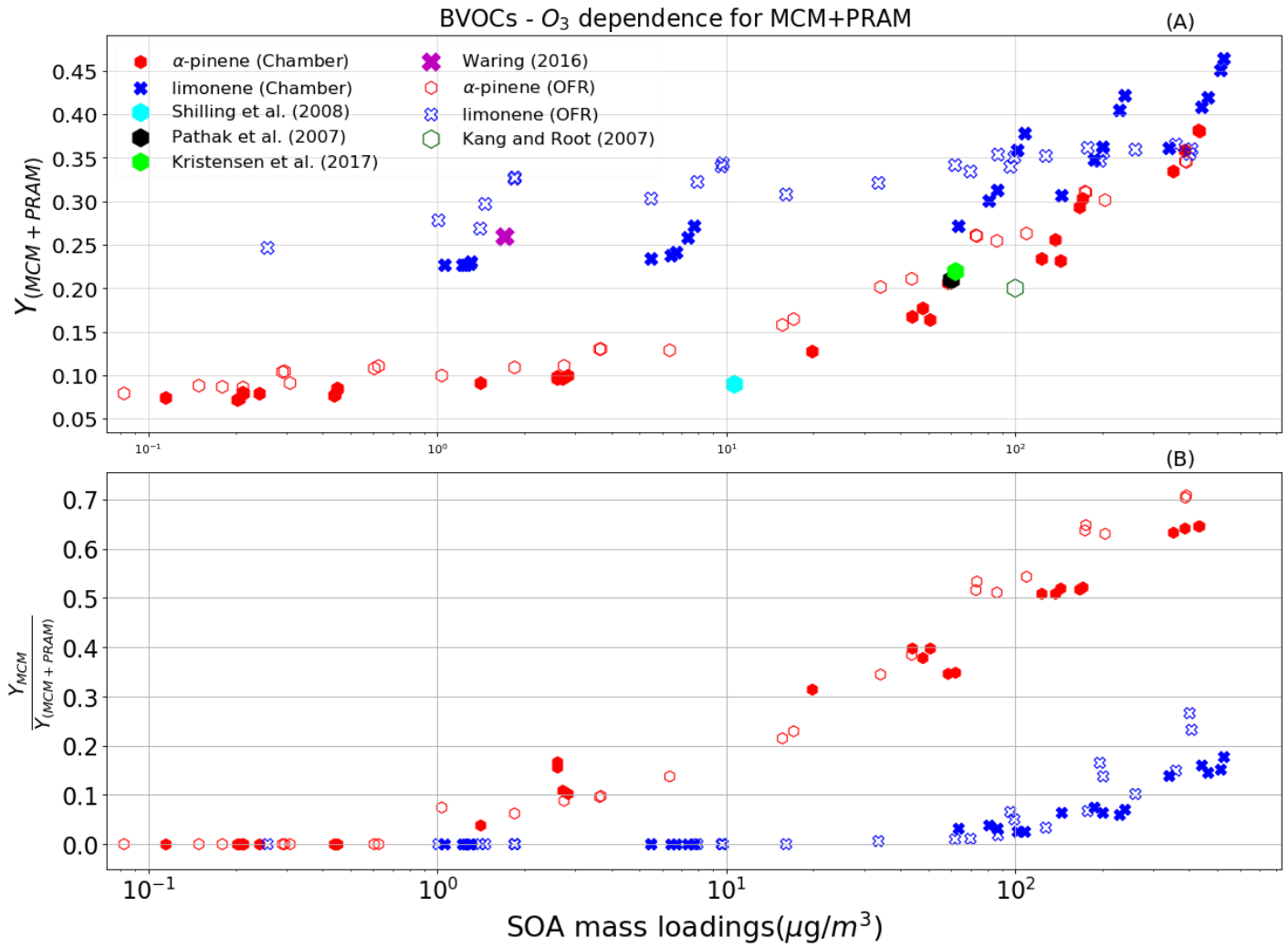

735 **Figure 1.** The mass yields from the ozonolysis of BVOCs α-pinene (red heptagon) and limonene (blue crosses) modelled after
736 chamber (filled symbols) and flow-tube settings (open symbols). The figure shows a comparison of SOA mass yields obtained from
737 simulations with MCM + PRAM (panel A) and ratio of yields from MCM and MCM+PRAM (panel B). Currently PRAM is
738 available for ozonlysis of limonene and α-pinene. The clumps are a result of SOA mass yields for the oxidation of specific oxidant
739 concentration with varying BVOC concentration

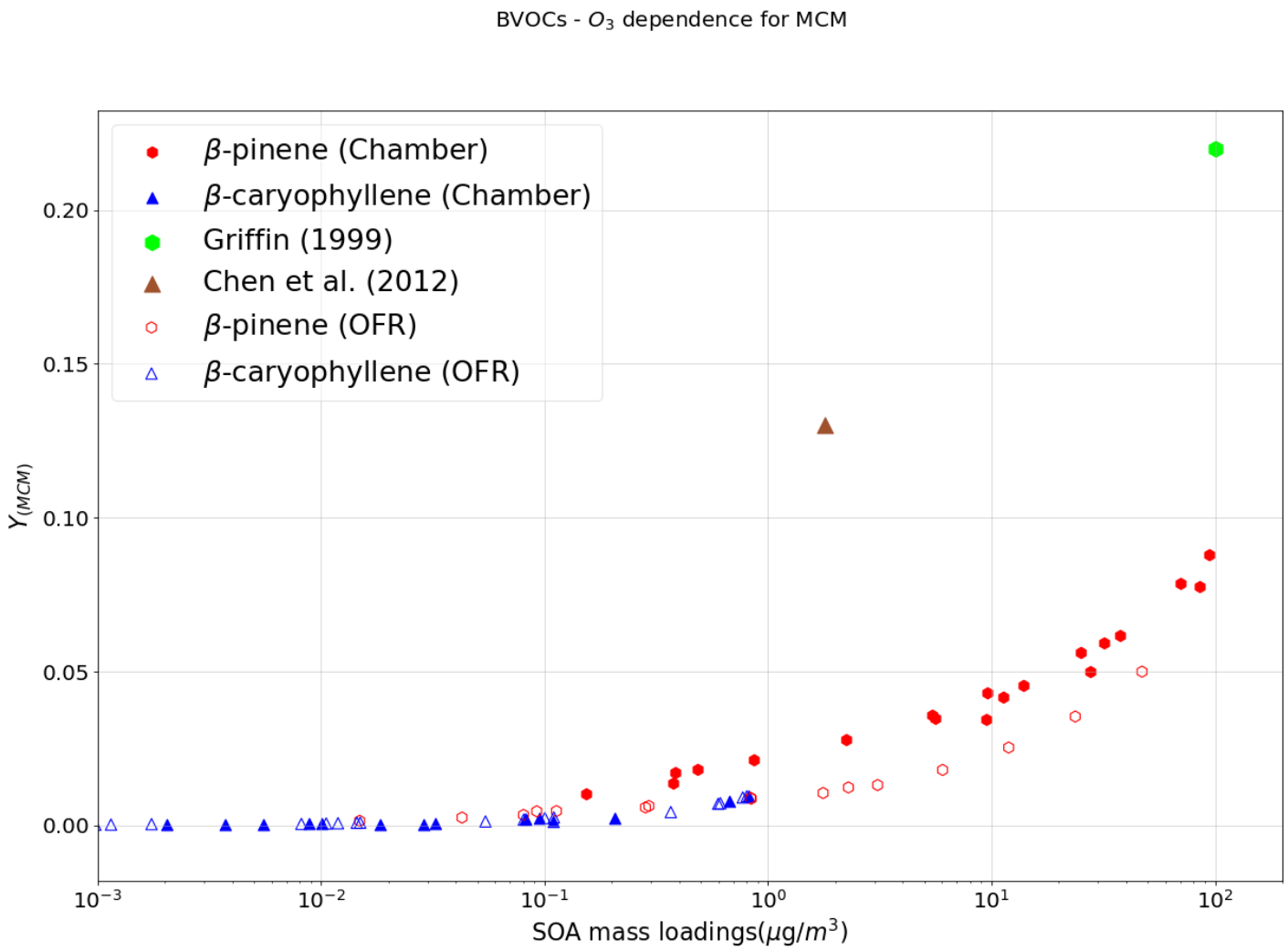

741 **Figure 2.** The mass yields from the ozonolysis of BVOCs β-pinene and β-caryophyllene modelled after chamber (filled symbols)
742 and flow-tube (open symbols) settings. The figure shows a comparison of SOA mass yields obtained from simulations with only
743 MCM as currently there is no PRAM available for these compounds. The experimental values are provided for comparison.

744 **3.2 BVOCs – OH chamber and flow-tube simulations**

745 The mass yields obtained by MCM+PRAM for α-pinene – OH oxidation are close to the measured
746 values (Kristensen et al., 2017), while using only MCM under-predicts the mass yields (Figure 3 , panel A
747 and B, and Table 3). The maximum SOA mass yield for OH oxidation of α-pinene is lower than the yield
748 from ozonolysis which is suspected to arise due to the formation of more volatile oxidation products produced
749 during OH oxidation (Bonn and Moortgat, 2002; Kristensen et al., 2014). The OH oxidation of β-pinene
750 results in mass yields similar to the measurements obtained by Lee et al. (2006b) for similar mass loadings.
751 The β-pinene SOA yields are comparatively well represented by MCM+PRAM in comparison to the
752 standalone MCM. On the other hand, the limonene mass yields are under-predicted by MCM+PRAM for

753 similar mass loadings. Yields for limonene SOA mass loadings of 350 µg m^{-3} are around 0.31 which is lower
754 than the experimental values, measured by Lee et al. (2006b).

755 For β-caryophyllene, the modeled values are in good agreement with experimental measured yields in
756 the range of mass loadings provided by Griffin (1999) and Tasoglou and Pandis (2015). Currently there are no
757 experiments providing HOM yields from OH oxidation of β-caryophyllene, and hence, those species are not
758 included in PRAM. The simulation results for yields from OH oxidation of β-caryophyllene, indicate that the
759 MCM scheme is able to reproduce the experimental values (Fig. 4). Only MCM was used for modeling the
760 mass yields for OH oxidation of isoprene due to current lack of PRAM mechanism for isoprene. The mass
761 yields derived from OH oxidation of isoprene vary from 0.01 - 0.31 covering a range of mass loadings from
762 0.003 - 132 µg m^{-3}. At low mass loadings < 10 µg m^{-3} the maximum yield obtained is ~0.06, which is a factor
763 of 3 greater than the experimental results obtained by (Lee et al., 2006b) where they measured yield of 0.02.
764 The mass yields are in good agreement with the experimental results from Liu et al. (2016), wherein they
765 measured a yield of 0.13 for 22 µg m^{-3} (Table 3).

766 The OFR simulations results for the OH oxidation of BVOCs with an equivalent exposure range from
767 2.0 x 10^{10} – 2.0 x 10^{12} molecules cm^{-3} s, is shown in Fig. 2. Our yields for α-pinene agree well with the yields
768 obtained by Bruns et al. (2015) where they measured yield of ~0.3 for mass loading of ~300 µg m^{-3} at
769 equivalent OH exposures. Friedman and Farmer (2018) found mass yields of 0 - 0.086 for α-pinene
770 (ammonium sulfate seeded experiment), 0- 0.12 for β-pinene (no seed particles) and 0-0.04 for limonene (no
771 seed particles), by varying the OH exposures between 4.7 x 10^{10} – 7.4 x 10^{11} molecules cm^{-3} s. Our simulated
772 yields for OH oxidation of α-pinene, β-pinene and limonene suggest higher mass yields for α-pinene and
773 limonene at equivalent mass loadings, while mass yields for β-pinene are in good agreement with the
774 experimental yields. Friedman and Farmer (2018) suggest that the reason for this underestimation in mass
775 yields could arise due to the exclusion of large particle sizes in the experiments and propose that these yields
776 could represent lower bounds.

777 **Table 3.** Mass yields for OH oxidation of BVOCs at 293 K for different range of mass loadings using a
778 chamber[†] and OFR[‖] setup.

SOA mass loading (µg m^{-3})	**MCM + PRAM mass yields**	**MCM mass yields**	**BVOC**	**Experimental yields**	**References**
300[†]	0.28	0.25	β-pinene	0.31 (293)	Lee et al. (2006b)

350†	0.31	0.06 – 0.11	limonene	0.58 (394)	Lee et al. (2006b)
30	0.09	0.004	α-pinene	0.11 (30)	Kristensen et al., 2017
< 10† 20 – 80†	0.21‼ 0.3 – 0.7‼	0.21 0.3 – 0.7	β-caryophyllene	0.2 (8.8) 0.37 – 0.79 (17-82)	Tasoglou and Pandis (2015) Griffin (1999)
22† <10	0.1‼ 0.06‼	0.1 0.06	Isoprene	0.13 (22) 0.02 (9)	Liu et al. (2016) Lee et al. (2006b)
0-300‖	0.05 – 0.31	0 – 0.2	α-pinene	0 – 0.086 (0 -300) 0.3 (300)	Friedman and Farmer (2018) Bruns et al. (2015)
0-30‖	0-0.1	0-0.01	β-pinene	0 – 0.12 (30)	Friedman and Farmer (2018)
0-40‖	0.-0.19	0-0.17	limonene	0.0 – 0.04 (35)	Friedman and Farmer (2018)

779 "indicates that no PRAM mechanism available yet i.e the yields are same as the MCM yields.

780

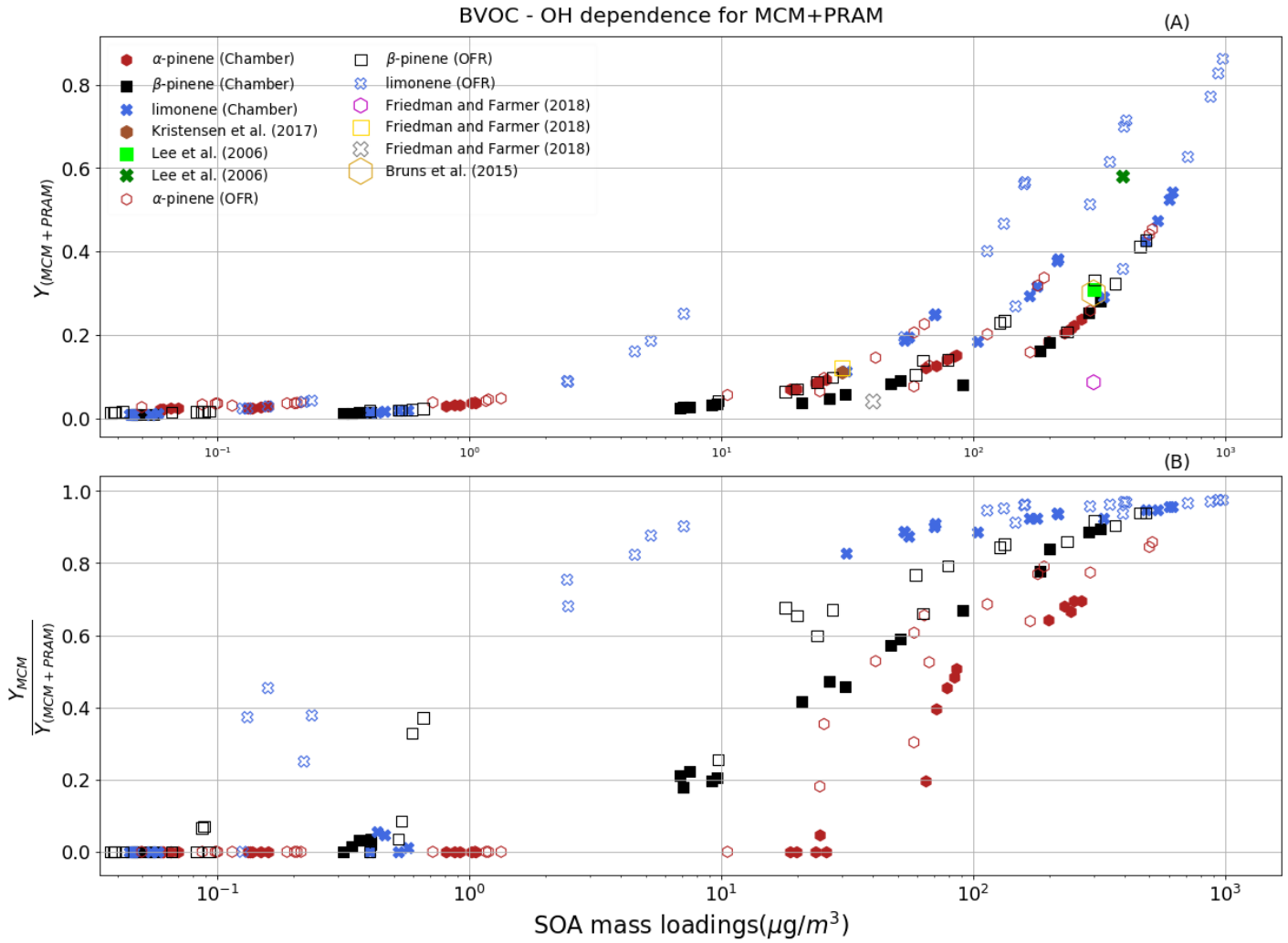

781 **Figure 3.** The mass yields from OH oxidation of BVOCs α-pinene (red heptagons), β-pinene (black squares) and limonene (blue
782 crosses) modeled after chamber (filled symbols) and flow-tube settings (open symbols). The figure shows a comparison of SOA
783 mass yields obtained from application of MCM+PRAM (panel A) and ratio of yields from MCM and couple MCM+PRAM (panel
784 B). Currently PRAM is available for OH oxidation of limonene and α-pinene and β-pinene.

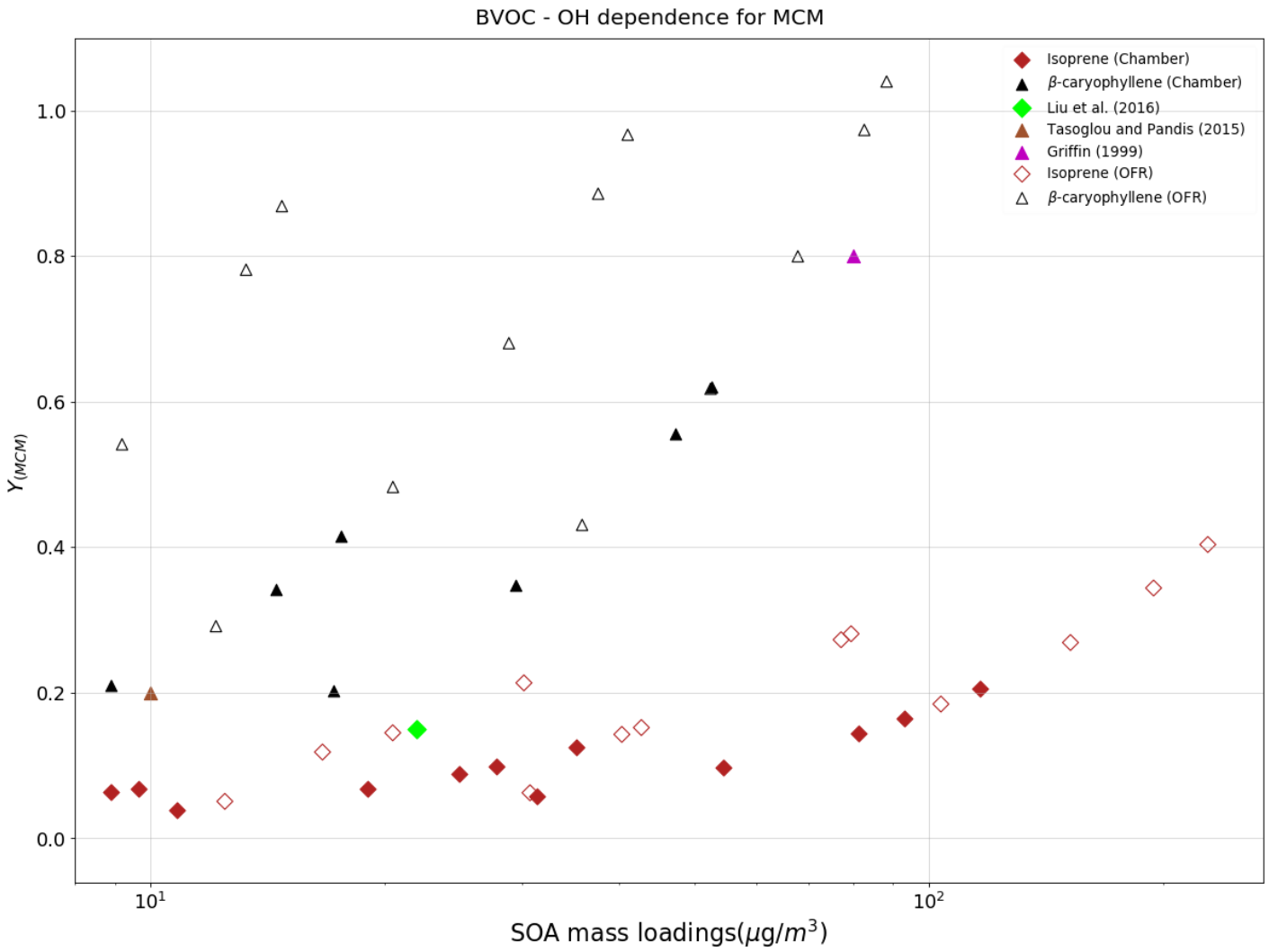

786 **Figure 4.** The mass yields from OH oxidation of BVOCs β-caryophyllene (black triangles) and isoprene (maroon diamonds)
787 modeled after chamber (filled symbols) and flow-tube settings (open symbols). The figure shows a comparison of SOA mass yields
788 obtained from application of MCM as currently there is no PRAM available for these compounds.

789 ### 3.3 BVOC – NO_3 chamber and OFR simulations

790 Figure 5. shows the yields derived from the oxidation of BVOCs by NO_3. Currently, as no PRAM is
791 available for NO_3 oxidation, Figure 5 represents SOA yields derived using MCM. Due to limited
792 experimental constraints, PRAM presently does not consider autoxidation of RO_2 formed from NO_3 oxidation
793 of VOCs,which could explain the huge discrepancy between the measured and simulated mass yields (Figure
794 5). The yields obtained for oxidation of α-pinene (0.002-0.007) by NO_3 are low in comparison to those
795 obtained by Nah et al. (2016), where they measured a yield of 0.036. Measured mass yields for limonene
796 oxidation by NO_3 resulting in mass yields between 0.25-0.4 (Fry et al., 2011), whereas we obtain negligible
797 (~0.0003) mass yields for the same.

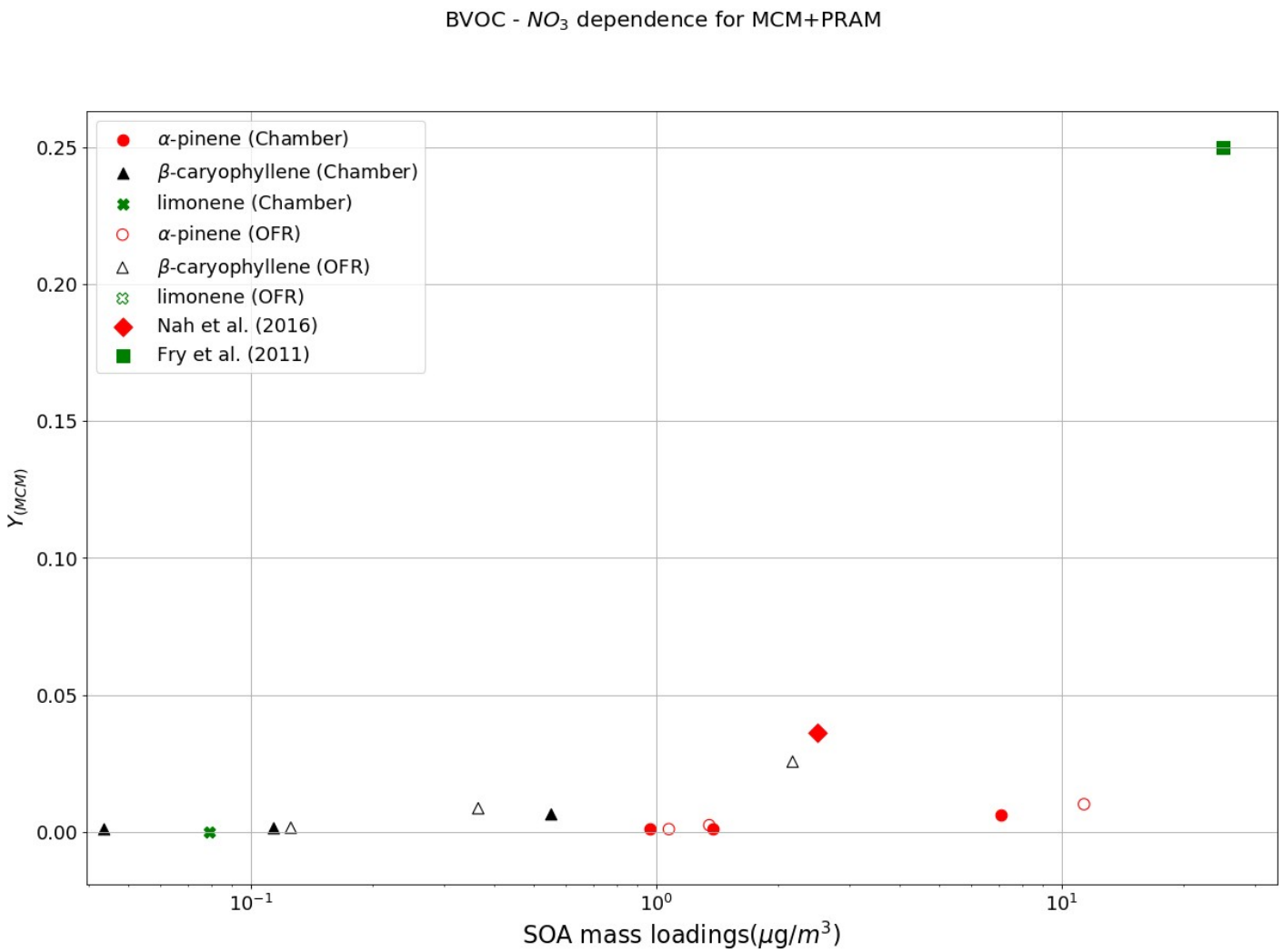

798 **Figure 5.** The mass yields from NO_3 oxidation of BVOCs modeled after chamber and flow-tube settings. The figure shows a
799 comparison of SOA mass yields obtained from application of MCM+PRAM. Appreciable mass yields were only obtained for α-
800 pinene, limonene and β-caryophyllene.

801 ## 3.4 NO_x dependence

802 Varying NO_x concentrations changes the fate of RO_2 radical formed during organic oxidations by
803 altering HO_2/RO_2 ratio, thereby impacting the distribution of reaction products and aerosol formation (Presto
804 et al., 2005; Zhao et al., 2018; Sarrafzadeh et al., 2016). We modeled the SOA mass yields for α-pinene - O_3
805 setup with varying NO_x concentrations (NO was varied whereas NO_2 was kept constant for all the runs), for
806 initial α-pinene mixing ratios in the range 0.5 - 200 ppb (Fig. 6). A maximum SOA yield value of 0.55 is
807 obtained for a combination of the lowest value of NO (0 ppb, red circles). As the NO concentrations increase
808 from 0.2 ppb (blue squares) to 5 ppb (green inverted triangles) the yields begin to decrease, and this pattern is
809 observable and valid for all concentration ranges of reacted precursor VOC. The NO_x dependence of α-pinene

ozonolysis is consistent with the findings of Draper et al. (2015) and Presto et al. (2005) wherein they observed a trend of decreasing SOA mass yields for α-pinene ozonolysis with increasing NO_x concentrations.

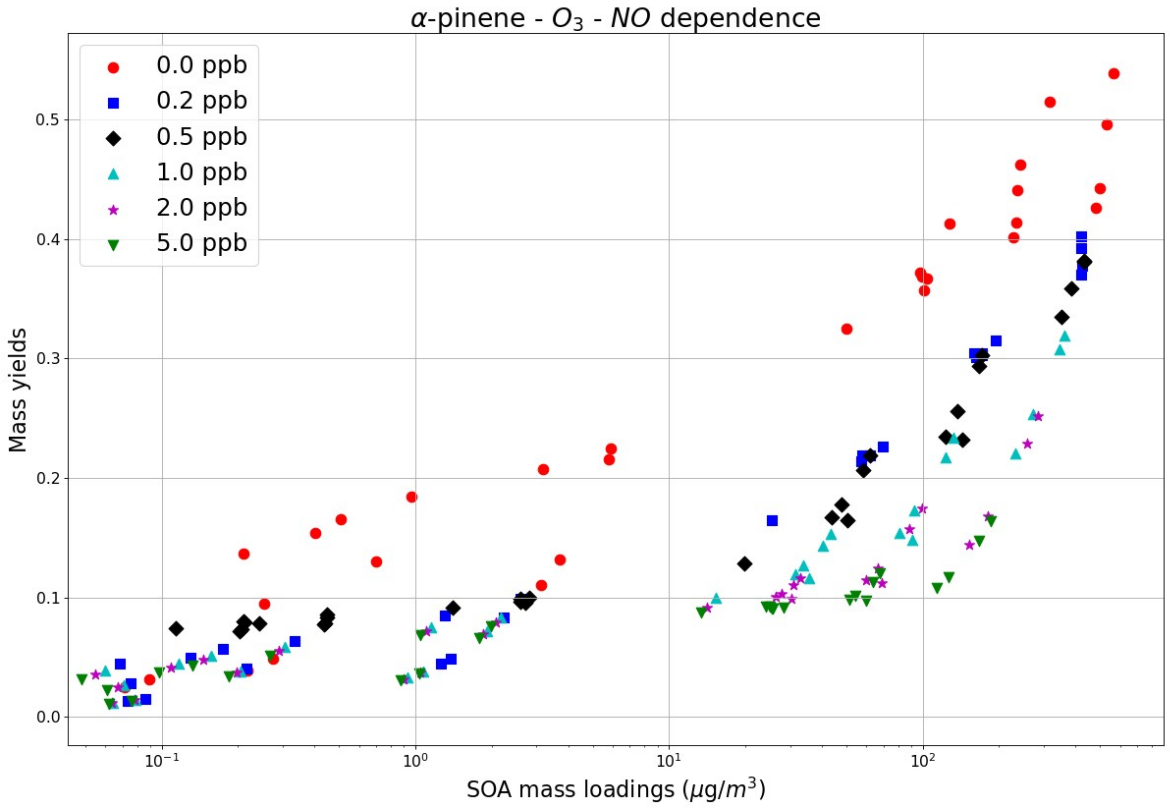

Figure 6. The SOA mass yields from O_3 oxidation of α-pinene modeled for different NO concentrations with the chamber setup. The model runs were performed using MCM+PRAM.

At low NO_x concentrations RO_2 radicals undergo rapid autoxidation until they react with HO_2 or RO_2 resulting in production of low volatility hydro-peroxide products (Sarrafzadeh et al., 2016), closed shell monomers or dimers (Ehn et al., 2014; Roldin et al., 2019), which increase SOA mass. This contrasts with high NO_x conditions where the RO_2+NO reactions dominate over reactions with HO_2 or RO_2, resulting in the formation of more volatile products such as aldehydes, ketones and organonitrates (Presto et al., 2005; Sarrafzadeh et al., 2016), and likely suppressing the autoxidation process leading to a decrease in SOA mass loadings (Ehn et al., 2014).

Figure 7 shows the absolute contributions to SOA mass loadings by PRAM and MCM compounds at two different O_3 concentrations of 4 and 100 ppb and varying NO concentrations. The figure shows that with an increase in NO concentrations the contribution of PRAM compounds to the particle phase decreases at

both 4 and 100 ppb of O_3 concentrations. In PRAM the RO_2 + NO reaction leads either to the formation of organonitrate HOM, closed shell monomers with carbonyl group or fragmentation products with higher volatility (Roldin et al., 2019). HOM Dimer formation is suppressed with increasing NO concentrations in PRAM (Roldin et al., 2019) which explains the lower contribution by PRAM compounds to SOA mass loadings with increasing NO. At NO concentrations <1ppb the PRAM contribution increases as, first generation RO_2 are capable of undergoing autoxidation forming highly oxygenated RO_2 which subsequently reacts with NO forming organic nitrates (Ehn et al., 2014). As NO concentrations exceed 1ppb the first generation RO_2 is scavenged by NO thereby reducing the concentration of organonitrate HOM (Ehn et al., 2014), possibly affecting SOA yields. The MCM contribution also decreases with increasing NO concentrations mostly due to the formation of more volatile organonitrates (Jenkin et al., 2019) .

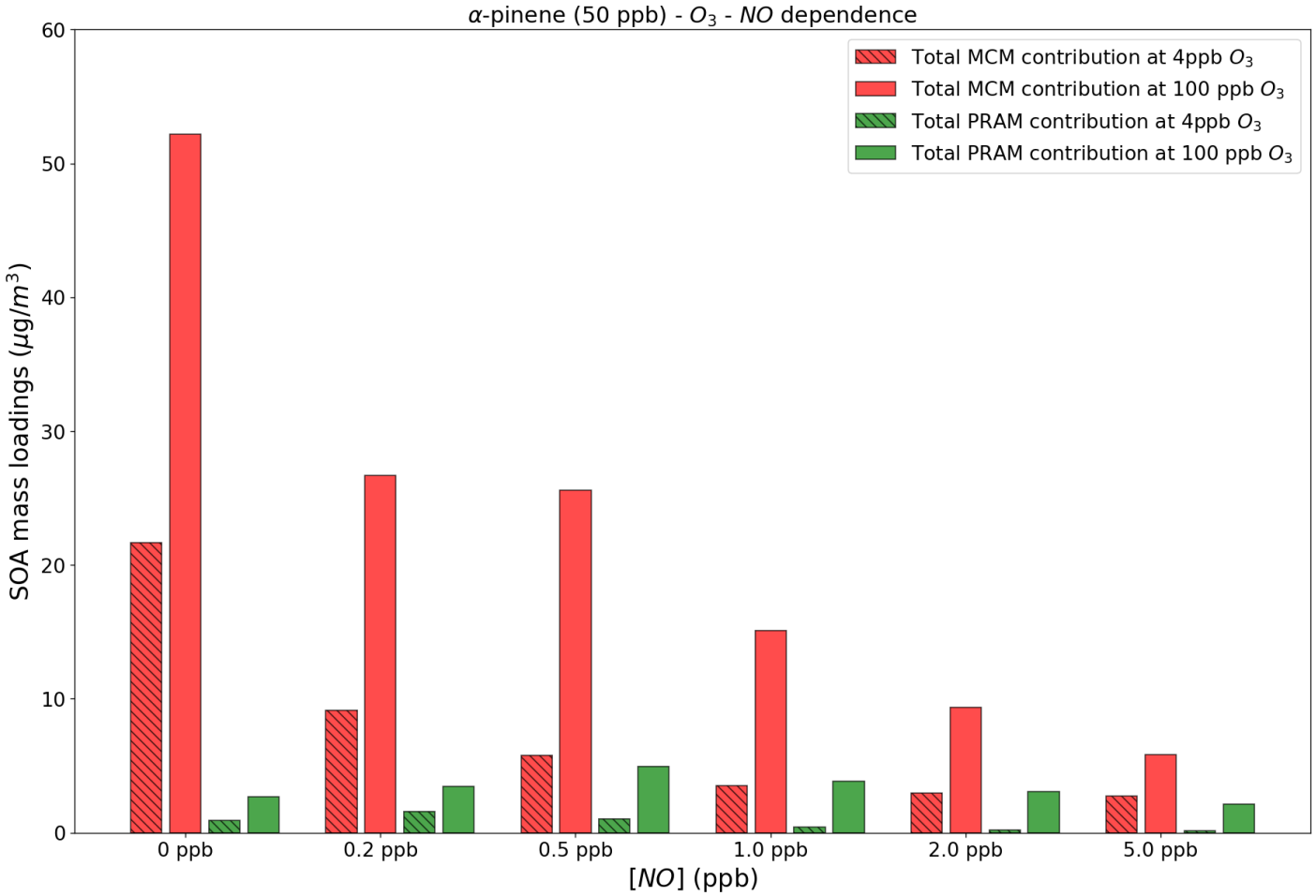

Figure 7. Contribution to the SOA mass loadings by total PRAM and MCM compounds at different NO_x levels and O_3 concentrations. For comparison we use 4 ppb and 100 ppb O_3 concentrations, respectively, at 50 ppb α-pinene.

838 **3.5 Temperature dependence**

839 The formation of SOA from α-pinene ozonolysis in the temperature range of 258.15 - 313.15 K was
840 investigated in this study using MCM+PRAM. Strong dependence of SOA mass yield on temperature was
841 reported by Saathoff and Naumann, (2009) wherein they measured the decreasing mass yields from 0.42 at
842 273.15 K to 0.09 to 313.15 K for SOA loadings of 53 and 92 μgm^{-3} respectively. Our results in Figure 8
843 show increasing SOA mass yields for α-pinene ozonolysis with decreasing temperature, which is attributed to
844 the augmented condensation of oxidation products termed as semi volatile organic compounds (SVOC)
845 (Kristensen et al., 2017) at lower temperatures.

846 For α-pinene maximum mass loading < 150 μgm^{-3} the mass yields reach a maximum value of 0.38 at
847 temperatures as low as 258.15 K and decrease to 0.27 for a temperature of 293.15 K and to 0.1 for the
848 temperature of 313.15 K. These yields are comparable to the results obtained by Kristensen et al.
849 (2017) where they measured yields of 0.39 for 258.15 K and 0.22 for 293.15 K for mass loading < 150 μgm^{-3}.
850 The results show a weak dependence of SOA mass yields on temperatures in the range of 278.15 K - 313.15
851 K at low SOA mass loadings which become more pronounced as the mass loadings increase. At the lowest
852 temperature of 258.15 K the mass yields are higher in comparison to other temperatures regardless the mass
853 loadings. These results are in good agreement with the findings by Pathak et al. (2007) where they found a
854 strong temperature dependence of SOA mass yields at lower temperature (0 – 15^{o} C), which decreases as the
855 temperature increases. Furthermore, similar to the measurements made by Pathak et al. (2007), our
856 simulations were able to reproduce the experimental findings that show no appreciable differences in the SOA
857 mass yields for loadings below 1 μgm^{-3} (initial mixing ratio of 1 ppb) for temperatures > 273.15 K.

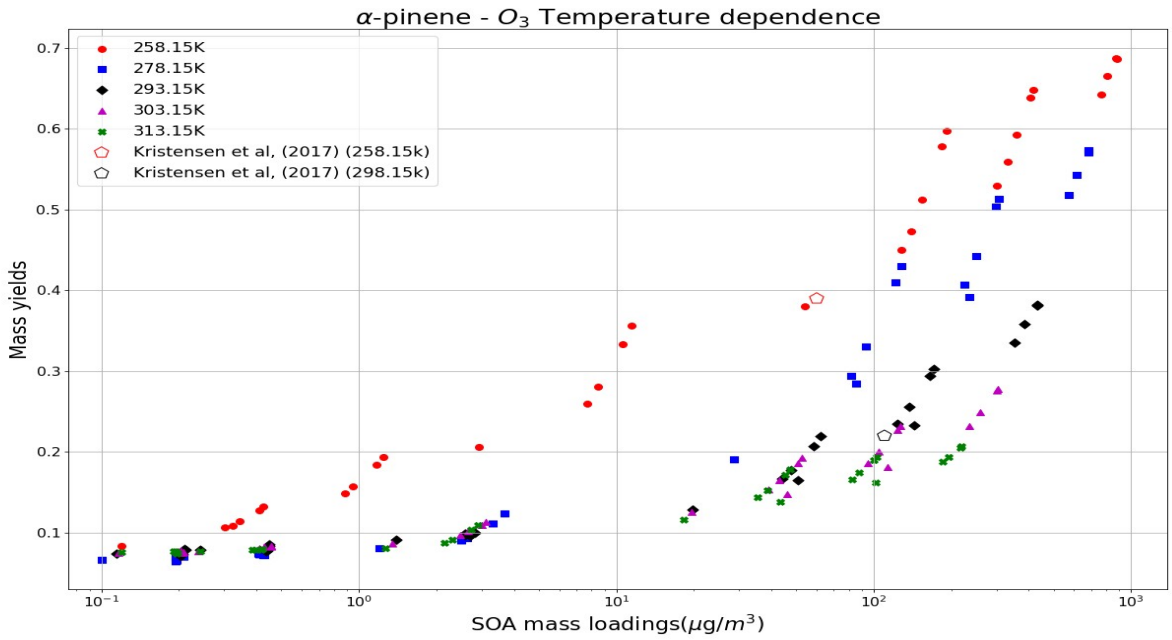

Figure 8. Temperature dependence of SOA mass yields at different temperatures using the MCM+PRAM. The open pentagons represent measurement data from Kristensen et al. (2017) at 258.15 K and 298.15 K.

Figure 9 shows the volatility distribution of α-pinene ozonolysis derived SOA at different temperatures. The saturation vapor pressure limits for defining extremely low volatility (ELVOCs - grey shaded), low volatility (LVOCs - red shaded), semi volatile (SVOCs - green shaded) and intermediate volatility (IVOCs - cyan shaded) organic compounds used in the Volatility basis set (VBS) are set according to the values suggested in Donahue et al. (2012). In this work, we categorize compounds (ELVOCs, LVOCs, SVOCs and IVOCs) based on effective saturation vapor pressures (C*) in the range of $\{10^{-5}$ to $10^{3}\}$ μgm^{-3} and temperature of 298 K (Donahue et al., 2009). At the lowest temperature of 258.15 K, the SVOCs contribution to the particle phase is dominant in comparison to LVOCs and ELVOCs, a trend which is subsequently reversed as the temperatures are increased. At 293.15 K a majority of SVOCs and IVOCs are in the gas phase while the contribution of LVOCs and ELVOCs to particle phases increases. These results are in good agreement with observations made by Kristensen et al. (2017) wherein they observed an increasing contribution of SVOCs at sub-zero temperatures of 258.15 K, which decrease the fraction of SOA formed from ELVOCs. Again, it should be noted that the temperature dependence of peroxy radical autoxidation product formation still needs further validation based on recent experiments (e.g. Quéléver et al., 2018).

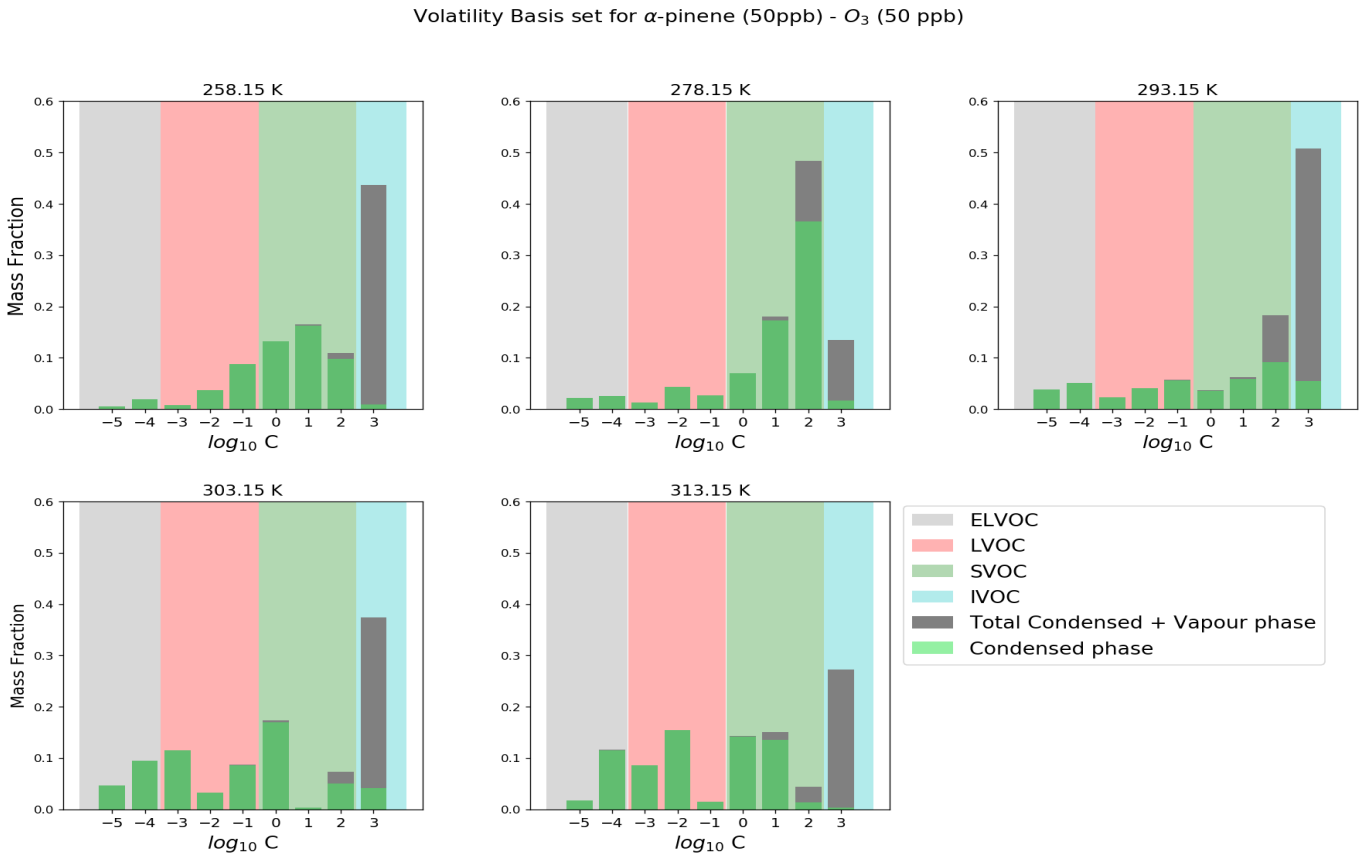

Figure 9. Modeled volatility distribution of SOA at different temperatures. The volatility bins span a range of effective saturation vapor pressures C = C* = {10^{-5} to 10^{3}} µgm^{-3}. The VBS distribution is based on a reference temperature of 298 K.

3.6 Composition

MCM+PRAM can be used to narrow down and compile a list of compounds playing a pivotal role in contributing to SOA mass loadings and, also compare the relative importance of implementing PRAM alongside the MCM. Figure 10 shows the most important compounds from both the MCM and PRAM that together contribute to more than 95% of α-pinene ozonolysis SOA mass loading at 293.15 K.

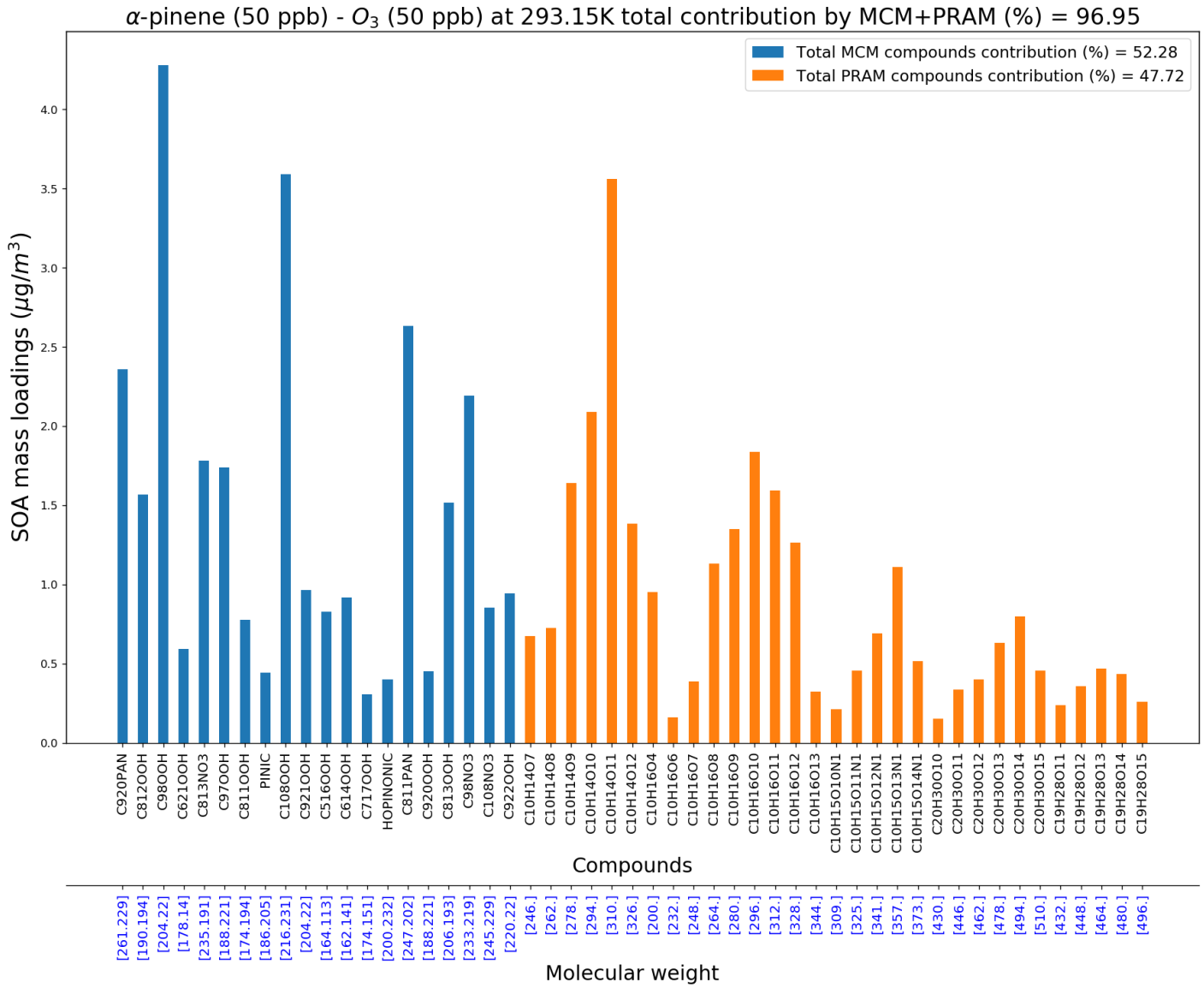

Figure 10. MCM and PRAM Compounds contributing to > 95 % of SOA mass at 293 K and 50ppb O_3 and α-pinene concentrations.

Figure 10 shows that contribution to SOA mass loadings by PRAM compounds is ~48 % (of 97 %) while MCM compounds contribute ~52 % (of 97%). On lowering the temperature to 258K the relative contributions of PRAM drop to 15 % (of ~98 %), while MCM dominates by contributing ~85 % (of ~98 %) respectively (Figure S3a). The contribution of PRAM increases to ~64 % (of ~97 %) and MCM contribution drops to 36 % (of ~97 %) at 313 K (Figure S3b). These results reflect the importance of PRAM as its contribution plays an increasingly dominant role with increasing temperatures and highlights the crucial few compounds that contribute to maximum SOA mass loadings for α-pinene ozonolysis. The list of abundant compounds which together add up to contribute more than 95 % of SOA mass loadings at 258 K, 293 K and 313 K are presented in the supplement Table 1s (a, b & c). At 258 K MCM compounds namely pinonic acid ($C_{10}H_{16}O_3$, 4.4 %),

C920PAN ($C_{10}H_{15}NO_7$, 9.3 %), C108NO3 ($C_{10}H_{15}NO_6$, 8.9 %), C811PAN ($C_9H_{13}NO_7$, 10.1 %), C717NO3 ($C_7H_9NO_6$, 11.3 %) contribute significantly to the total SOA mass loadings while PRAM compounds such as $C_{10}H_{14}O_7$ (0.88 %), $C_{10}H_{16}O_4$ (1.3 %), $C_{10}H_{16}O_6$ (1.13 %) contribute significantly less. An increase in temperature to 293 K results in an overall increase in contribution by PRAM compounds, with $C_{10}H_{14}O_{10}$ (3.6 %), $C_{10}H_{14}O_{11}$ (6.2 %), $C_{10}H_{16}O_{10}$ (3.2 %) playing an important role in contributing to the SOA mass loadings. This trend of relative increase in the contribution by PRAM compounds over MCM compounds to SOA mass loadings is also evident as the temperatures are further increased to 313 K, where the PRAM compounds $C_{10}H_{14}O_{11}$ (18.3 %), $C_{10}H_{14}O_{12}$ (6 %) and $C_{10}H_{16}O_{12}$ (6.6 %) play a dominant role in increasing SOA mass loadings.

4. Conclusions

We simulated SOA mass yields derived from the oxidation of various BVOCs (isoprene, α-pinene, β-pinene, limonene and β-caryophyllene), by the oxidants O_3, OH and NO_3 using the zero-dimensional model MALTE-Box. The gas phase chemistry was simulated using the MCM in conjunction with PRAM. The aim was to verify the efficacy of MCM+PRAM in simulating the SOA mass yields. Additional simulations were performed to test the MCM+PRAM under varying temperature and NO concentrations. A few important compounds playing a major role in increasing the SOA mass yields for α-pinene ozonolysis at different temperatures are also highlighted.

The simulations were designed to resemble ideal smog chambers experiments and experiments in oxidative flow reactors (OFR). No interactions between the gas phase and chamber walls were considered during the simulations. For the smog chamber setting, the standalone MCM generally under-predicts the mass yields obtained by the ozonolysis and OH oxidation of BVOCs. In contrast, the yields derived using MCM+PRAM for the smog chamber setup is in good agreement with the experimental results. For an idealized OFR setup, MCM+PRAM yields are in good agreement with experimental yields, while again the MCM under-predicts the SOA yields. The relative contribution of HOM monomers and dimers to the particle phase in OFR simulations is low when compared to the chamber simulations. This is due to higher RO_2 concentrations in OFR leading to termination of peroxy radical autoxidation, thereby affecting SOA yields. This needs to be considered when applying yields based on OFR simulations in regional or global chemical transport models

The model does not simulate appreciable SOA mass yields for oxidation of BVOCs with NO_3, as PRAM currently does not consider autoxidation of RO_2 formed from NO_3 oxidation of VOCs. This underlines the need for developing a NO_3 oxidation scheme which can better constrain and predict SOA mass yields. In

accordance to the previous studies, the simulated SOA yields tend to decrease at higher temperatures. The PRAM contribution to mass yields at low temperatures (258.15 K) is ~14 %, which is substantially lower than that of MCM (~86 %). As the temperature is increased to 313.15 K, the contribution of PRAM to SOA mass yields begins to dominate over MCM. This most likely is due to MCM producing more SVOCs (compounds classified as SVOCs at 298 K), which show stronger contribution to particle phase at lower temperatures, due to decrease in saturation vapor pressures with temperature. It should be noted that the present temperature dependency of mass yields using PRAM are a first, and currently the best estimate in understanding the influence of temperature on the peroxy radical autoxidation formation. The simulated SOA yields with varying NO concentrations agree well with experimental results, i.e. SOA yields decrease with increasing NO concentrations due to the formation of more volatile compounds such as organonitrates and ketones.

Using PRAM coupled with MCM helps us bridge the gap in understanding the role and contribution of peroxy radical autoxidation to SOA formation. The variation of SOA yields for temperature and NO concentrations, indicates the limitations of global and regional models in predicting e.g. cloud condensation nuclei (CCN) effects using fixed SOA yields. The good agreement of modeled and experimental yields from smog chambers, could further help us parameterize the SOA yields, that could be applied at a global and regional model scale, to more accurately predict the direct and indirect impact of aerosol particles on e.g. radiation balance by aerosol scattering/absorption and CCN concentrations. Furthermore, implementation of a condensed PRAM version to regional and global models has been tested but still need further validation (Roldin et al., 2019).

Data availability

The complete PRAM mechanism written in a format compatible with the Kinetic PreProcessor (KPP) together with all species information can also be downloaded from https://doi.org/10.1594/PANGAEA.905102

Author Contributions

CX and MB served as the chief authors and editors of the paper. CX was performing the model simulations. The study was designed by CX, MB and PR. All other co-authors contributed to the analysis and writing of the paper.

Acknowledgements

The presented research has been funded by the Academy of Finland (Center of Excellence in Atmospheric Sciences) grant no. 4100104 and the Swedish Research Council FORMAS, project no. 2018-01745. We would also like to acknowledge the invaluable contribution of computational resources from CSC – IT Center for Science, Finland.

References

Ahlberg, E., Eriksson, A., Brune, W. H., Roldin, P. and Svenningsson, B.: Effect of salt seed particle surface area, composition and phase on secondary organic aerosol mass yields in oxidation flow reactors, Atmos. Chem. Phys., 19(4), 2701–2712, doi:10.5194/acp-19-2701-2019, 2019.

Berndt, T., Richters, S., Jokinen, T., Hyttinen, N., Kurtén, T., Otkjær, R. V., Kjaergaard, H. G., Stratmann, F., Herrmann, H., Sipilä, M., Kulmala, M. and Ehn, M.: Hydroxyl radical-induced formation of highly oxidized organic compounds, Nat. Commun., 7(May), doi:10.1038/ncomms13677, 2016.

Bianchi, F., Garmash, O., He, X., Yan, C., Iyer, S., Rosendahl, I., Xu, Z., Rissanen, M. P., Riva, M., Taipale, R., Sarnela, N., Petäjä, T., Worsnop, D. R., Kulmala, M., Ehn, M. and Junninen, H.: The role of highly oxygenated molecules (HOMs) in determining the composition of ambient ions in the boreal forest, Atmos. Chem. Phys., 17(22), 13819–13831, doi:10.5194/acp-17-13819-2017, 2017.

Bianchi, F., Kurtén, T., Riva, M., Mohr, C., Rissanen, M. P., Roldin, P., Berndt, T., Crounse, J. D., Wennberg, P. O., Mentel, T. F., Wildt, J., Junninen, H., Jokinen, T., Kulmala, M., Worsnop, D. R., Thornton, J. A., Donahue, N., Kjaergaard, H. G. and Ehn, M.: Highly Oxygenated Organic Molecules (HOM) from Gas-Phase Autoxidation Involving Peroxy Radicals: A Key Contributor to Atmospheric Aerosol, Chem. Rev., doi:10.1021/acs.chemrev.8b00395, 2019.

Bonn, B. and Moortgat, G. K.: New particle formation during α- and β-pinene oxidation by O3, OH and NO3, and the influence of water vapour: Particle size distribution studies, Atmos. Chem. Phys., 2(3), 183–196, doi:10.5194/acp-2-183-2002, 2002.

Boy, M., Hellmuth, O., Korhonen, H., Nilsson, E. D., Revelle, D., Turnipseed, A., Arnold, F. and Kulmala, M.: MALTE - Model to predict new aerosol formation in the lower troposphere, Atmos. Chem. Phys., 6(12), 4499–4517, doi:10.5194/acp-6-4499-2006, 2006.

Bruns, E. A., El Haddad, I., Keller, A., Klein, F., Kumar, N. K., Pieber, S. M., Corbin, J. C., Slowik, J. G., Brune, W. H., Baltensperger, U. and Prévôt, A. S. H.: Inter-comparison of laboratory smog chamber and flow reactor systems on organic aerosol yield and composition, Atmos. Meas. Tech., 8(6), 2315–2332, doi:10.5194/amt-8-2315-2015, 2015.

Chen, Q., Li, Y. L., McKinney, K. A., Kuwata, M. and Martin, S. T.: Particle mass yield from β-caryophyllene ozonolysis, Atmos. Chem. Phys., 12(7), 3165–3179, doi:10.5194/acp-12-3165-2012, 2012.

Crounse, J. D. and Nielsen, L. B.: Autoxidation of Organic Compounds in the Atmosphere, J. Phys. Chem. Lett., 24(4), 3513–3520, doi:10.1021/jz4019207, 2013.

Damian, V., Sandu, A., Damian, M., Potra, F. and Carmichael, G. R.: The kinetic preprocessor KPP - A software environment for solving chemical kinetics, Comput. Chem. Eng., 26(11), 1567–1579, doi:10.1016/S0098-1354(02)00128-X, 2002.

Donahue, N. M., Robinson, A. L., Stanier, C. O. and Pandis, S. N.: Coupled Partitioning, Dilution, and Chemical Aging of Semivolatile Organics, Environ. Sci. Technol., 40(8), 2635–2643, doi:10.1021/es052297c, 2006.

Donahue, N. M., Robinson, A. L. and Pandis, S. N.: Atmospheric organic particulate matter: From smoke to secondary organic aerosol, Atmos. Environ., 43(1), 94–106, doi:https://doi.org/10.1016/j.atmosenv.2008.09.055, 2009.

Donahue, N. M., Kroll, J. H., Pandis, S. N. and Robinson, A. L.: A two-dimensional volatility basis set-Part 2: Diagnostics of organic-aerosol evolution, Atmos. Chem. Phys., 12(2), 615–634, doi:10.5194/acp-12-615-2012, 2012.

Draper, D. C., Farmer, D. K., Desyaterik, Y. and Fry, J. L.: A qualitative comparison of secondary organic aerosol yields and composition from ozonolysis of monoterpenes at varying concentrations of NO2, Atmos. Chem. Phys., 15(21), 12267–12281, doi:10.5194/acp-15-12267-2015, 2015.

Ehn, M., Kleist, E., Junninen, H., Petäjä, T., Lönn, G., Schobesberger, S., Dal Maso, M., Trimborn, A., Kulmala, M., Worsnop, D. R., Wahner, A., Wildt, J. and Mentel, T. F.: Gas phase formation of extremely oxidized pinene reaction products in chamber and ambient air, Atmos. Chem. Phys., 12(11), 5113–5127, doi:10.5194/acp-12-5113-2012, 2012.

Ehn, M., Thornton, J. A., Kleist, E., Sipilä, M., Junninen, H., Pullinen, I., Springer, M., Rubach, F., Tillmann, R., Lee, B., Lopez-Hilfiker, F., Andres, S., Acir, I. H., Rissanen, M., Jokinen, T., Schobesberger, S., Kangasluoma, J., Kontkanen, J., Nieminen, T., Kurtén, T., Nielsen, L. B., Jørgensen, S., Kjaergaard, H. G., Canagaratna, M., Maso, M. D., Berndt, T., Petäjä, T., Wahner, A., Kerminen, V. M., Kulmala, M., Worsnop, D. R., Wildt, J. and Mentel, T. F.: A large source of low-volatility secondary organic aerosol, Nature, 506(7489), 476–479, doi:10.1038/nature13032, 2014.

Friedman, B. and Farmer, D. K.: SOA and gas phase organic acid yields from the sequential photooxidation of seven monoterpenes, Atmos. Environ., 187(January), 335–345, doi:10.1016/j.atmosenv.2018.06.003, 2018.

Fry, J. L., Kiendler-Scharr, A., Rollins, A. W., Brauers, T., Brown, S. S., Dorn, H. P., Dubé, W. P., Fuchs, H., Mensah, A., Rohrer, F., Tillmann, R., Wahner, A., Wooldridge, P. J. and Cohen, R. C.: SOA from limonene: Role of NO 3 in its generation and degradation, Atmos. Chem. Phys., 11(8), 3879–3894, doi:10.5194/acp-11-3879-2011, 2011.

Glasius, M. and Goldstein, A. H.: Recent Discoveries and Future Challenges in Atmospheric Organic Chemistry, Environ. Sci. Technol., 50(6), 2754–2764, doi:10.1021/acs.est.5b05105, 2016.

Griffin, R. J.: Organic aerosol formation from the oxidation of biogenic hydrocarbons, , 104(D3), 3555–3567, 1999.

Guenther, A., Baugh, B., Brasseur, G., Greenberg, J., Harley, P., Klinger, L., Serca, D., and Vierling, L.: Isoprene emission estimates and uncertainties for the Central African EXPRESSO study domain, J. Geophys. Res. Atmos., 104(D23), 30625–30639, doi:10.1029/1999JD900391, 1999.

Guenther, A., Nicholas Hewitt, C., David, E., Fall, R., Chris, G., Tom, G., Peter, H., Klinger, L., Manuel, L., Mckay, W. A., Tom, P., Scholes, B., Steinbrecher, R., Tallamraju, R., Taylor, J. and Zimmerman, P.: A global model of natural volatile organic compound emissions s Raja the balance Triangle changes in the atmospheric accumulation rates of greenhouse Triangle Several inventories of natural and Exposure Assessment global scales have been two classes Fores, J. Geophys. Res., 100(94), 8873–8892, doi:doi:10.1029/94JD02950, 1995.

Guenther, A., Geron, C., Pierce, T., Lamb, B., Harley, P. and Fall, R.: Natural emissions of non-methane volatile organic compounds, carbon monoxide, and oxides of nitrogen from North America, Atmos. Environ., 34(12–14), 2205–2230, doi:10.1016/S1352-2310(99)00465-3, 2000.

Hao, L. Q., Romakkaniemi, S., Yli-Pirilä, P., Joutsensaari, J., Kortelainen, A., Kroll, J. H., Miettinen, P., Vaattovaara, P., Tiitta, P., Jaatinen, A., Kajos, M. K., Holopainen, J. K., Heijari, J., Rinne, J., Kulmala, M., Worsnop, D. R., Smith, J. N. and Laaksonen, A.: Mass yields of secondary organic aerosols from the

oxidation of α-pinene and real plant emissions, Atmos. Chem. Phys., 11(4), 1367–1378, doi:10.5194/acp-11-1367-2011, 2011.

Henry, K. M., Lohaus, T. and Donahue, N. M.: Organic Aerosol Yields from α-Pinene Oxidation: Bridging the Gap between First-Generation Yields and Aging Chemistry, Environ. Sci. Technol., 46(22), 12347–12354, doi:10.1021/es302060y, 2012.

Jacobson, M. Z.: Numerical techniques to solve condensational and dissolutional growth equations when growth is coupled to reversible reactions, Aerosol Sci. Technol., 27(4), 491–498, doi:10.1080/02786829708965489, 1997.

Jenkin, M. E., Saunders, S. M. and Pilling, M. J.: The tropospheric degradation of volatile organic compounds: A protocol for mechanism development, Atmos. Environ., 31(1), 81–104, doi:10.1016/S1352-2310(96)00105-7, 1997.

Jenkin, M. E., Young, J. C. and Rickard, A. R.: The MCM v3.3.1 degradation scheme for isoprene, Atmos. Chem. Phys., 15(20), 11433–11459, doi:10.5194/acp-15-11433-2015, 2015.

Jenkin, M. E., Wyche, K. P., Evans, C. J., Carr, T., Monks, P. S., Alfarra, M. R., Barley, M. H., McFiggans, G. B., Young, J. C. and Rickard, A. R.: Development and chamber evaluation of the MCM v3.2 degradation scheme for β-caryophyllene, Atmos. Chem. Phys., 12(11), 5275–5308, doi:10.5194/acp-12-5275-2012, 2012.

Jenkin, M. E., Valorso, R., Aumont, B. and Rickard, A. R.: Estimation of rate coefficients and branching ratios for reactions of organic peroxy radicals for use in automated mechanism construction, Atmos. Chem. Phys. Discuss., (February), 1–46, doi:10.5194/acp-2019-44, 2019.

Jokinen, T., Berndt, T., Makkonen, R., Kerminen, V.-M., Junninen, H., Paasonen, P., Stratmann, F., Herrmann, H., Guenther, A. B., Worsnop, D. R., Kulmala, M., Ehn, M. and Sipilä, M.: Production of extremely low volatile organic compounds from biogenic emissions: Measured yields and atmospheric implications, Proc. Natl. Acad. Sci., 112(23), 7123–7128, doi:10.1073/pnas.1423977112, 2015.

Kanakidou, M., Seinfeld, J. H., Pandis, S. N., Barnes, I., Dentener, F. J., Facchini, M. C. and Dingenen, R. Van: Organic aerosol and global climate modelling: a review, , 1053–1123, 2005.

Kang, E. and Root, M. J.: Introducing the concept of Potential Aerosol Mass (PAM), Atmos. Chem. Phys., (7), 5727–5744

Keywood, M. D., Varutbangkul, V., Bahreini, R., Flagan, R. C. and Seinfeld, J. H.: Secondary organic aerosol formation from the ozonolysis of cycloalkenes and related compounds, Environ. Sci. Technol., 38(15), 4157–4164, doi:10.1021/es035363o, 2004.

Korhonen, H., Lehtinen, K. E. J. and Kulmala, M.: Atmospheric Chemistry and Physics Multicomponent aerosol dynamics model UHMA: model development and validation, Atmos. Chem. Phys, 4, 757–771, doi:10.1002/erv.2305, 2004.

Kristensen, K., Cui, T., Zhang, H., Gold, A., Glasius, M. and Surratt, J. D.: Dimers in α-pinene secondary organic aerosol: Effect of hydroxyl radical, ozone, relative humidity and aerosol acidity, Atmos. Chem. Phys., 14(8), 4201–4218, doi:10.5194/acp-14-4201-2014, 2014.

Kristensen, K., Jensen, L. N., Glasius, M. and Bilde, M.: The effect of sub-zero temperature on the formation and composition of secondary organic aerosol from ozonolysis of alpha-pinene, Environ. Sci. Process. Impacts, 19(10), 1220–1234, doi:10.1039/c7em00231a, 2017.

Kroll, J. H., Ng, N. L., Murphy, S. M., Flagan, R. C. and Seinfeld, J. H.: Secondary organic aerosol formation from isoprene photooxidation under high-NOxconditions, Geophys. Res. Lett., 32(18), 1–4, doi:10.1029/2005GL023637, 2005.

Lambe, A. T., Onasch, T. B., Massoli, P., Croasdale, D. R., Wright, J. P., Ahern, A. T., Williams, L. R., Worsnop, D. R., Brune, W. H. and Davidovits, P.: Laboratory studies of the chemical composition and cloud condensation nuclei (CCN) activity of secondary organic aerosol (SOA) and oxidized primary organic aerosol (OPOA), Atmos. Chem. Phys., 11(17), 8913–8928, doi:10.5194/acp-11-8913-2011, 2011.

Lambe, A. T., Chhabra, P. S., Onasch, T. B., Brune, W. H., Hunter, J. F., Kroll, J. H., Cummings, M. J., Brogan, J. F., Parmar, Y., Worsnop, D. R., Kolb, C. E. and Davidovits, P.: Effect of oxidant concentration, exposure time, and seed particles on secondary organic aerosol chemical composition and yield, Atmos. Chem. Phys., 15(6), 3063–3075, doi:10.5194/acp-15-3063-2015, 2015.

Lee, A., Goldstein, A. H., Keywood, M. D., Gao, S., Varutbangkul, V., Bahreini, R., Ng, N. L., Flagan, R. C. and Seinfeld, J. H.: Gas-phase products and secondary aerosol yields from the ozonolysis of ten different terpenes, J. Geophys. Res. Atmos., 111(7), 1–18, doi:10.1029/2005JD006437, 2006a.

Lee, A., Goldstein, A. H., Kroll, J. H., Ng, N. L., Varutbangkul, V., Flagan, R. C. and Seinfeld, J. H.: Gas-phase products and secondary aerosol yields from the photooxidation of 16 different terpenes, J. Geophys. Res. Atmos., 111(17), 1–25, doi:10.1029/2006JD007050, 2006b.

Liu, J., D'Ambro, E. L., Lee, B. H., Lopez-Hilfiker, F. D., Zaveri, R. A., Rivera-Rios, J. C., Keutsch, F. N., Iyer, S., Kurten, T., Zhang, Z., Gold, A., Surratt, J. D., Shilling, J. E. and Thornton, J. A.: Efficient Isoprene Secondary Organic Aerosol Formation from a Non-IEPOX Pathway, Environ. Sci. Technol., 50(18), 9872–9880, doi: 10.1021/acs.est.6b01872, 2016.

Miller, K. A., Siscovick, D. S., Sheppard, L., Shepherd, K., Sullivan, J. H., Anderson, G., L. and Kaufman J. D.: Long-Term Exposure to Air Pollution and Incidence of Cardiovascular Events in Women, N. Engl. J. Med., 356(5), 447–458, doi:10.1002/anie.201206370, 2007.

Nannoolal, Y., Rarey, J. and Ramjugernath, D.: Estimation of pure component properties part 3. Estimation of the vapor pressure of non-electrolyte organic compounds via group contribution and group interactions, Fluid Phase Equilib., 269(1–2), 117–133, doi: 10.1016/j.fluid.2008.04.020, 2008.

Nah, T., Sanchez, J., Boyd, C. M. and Ng, N. L.: Photochemical Aging of α-pinene and β-pinene Secondary Organic Aerosol formed from Nitrate Radical Oxidation, Environ. Sci. Technol., 50(1), 222–231, doi:10.1021/acs.est.5b04594, 2016.

Ng, N. L. and Chhabra, P. S.: Effect ofNOx level on secondary organic aerosol (SOA) formation from the photooxidation of terpenes, Atmos. Chem. Phys., (7), 5159–5174, doi: 10.1016/j.cub.2015.10.018, 2007.

Öström, E., Putian, Z., Schurgers, G., Mishurov, M., Kivekäs, N. and Lihavainen, H.: Modeling the role of highly oxidized multifunctional organic molecules for the growth of new particles over the boreal forest re-gion, , 8887–8901, 2017.

Pankow, J. F. and Asher, W. E.: SIMPOL.1: a simple group contribution method for predicting vapor pressures and enthalpies of vaporization of multifunctional organic compounds, Rev. Mex. Ciencias Farm., (8), 2773–2796, doi:doi: 10.5194/acp-8-2773-2008, 2008.

Pathak, R., Donahue, N. M. and Pandis, S. N.: Ozonolysis of β-pinene: Temperature dependence of secondary organic aerosol mass fraction, Environ. Sci. Technol., 42(14), 5081–5086, doi:10.1021/es070721z, 2008.

Pathak, R. K., Stanier, C. O., Donahue, N. M. and Pandis, S. N.: Ozonolysis of α-pinene at atmospherically relevant concentrations: Temperature dependence of aerosol mass fractions (yields), J. Geophys. Res. Atmos., 112(3), 1–8, doi:10.1029/2006JD007436, 2007.

Presto, A. A., Huff Hartz, K. E. and Donahue, N. M.: Secondary organic aerosol production from terpene ozonolysis. 2. Effect of NOx concentration, Environ. Sci. Technol., 39(18), 7046–7054, doi:10.1021/es050400s, 2005.

Qi, X., Ding, A., Roldin, P., Xu, Z., Zhou, P., Sarnela, N., Nie, W., Huang, X., Rusanen, A., Ehn, M., Rissanen, M. P., Petäjä, T., Kulmala, M. and Boy, M.: Modelling studies of HOMs and their contributions to new particle formation and growth: Comparison of boreal forest in Finland and a polluted environment in China, Atmos. Chem. Phys., 18(16), 11779–11791, doi:10.5194/acp-18-11779-2018, 2018.

Quéléver, L. L. J., Kristensen, K., Jensen, L., Rosati, B., Teiwes, R., Daellenbach, K. R., Peräkylä, O., Roldin, P., Pedersen, H. B., Glasius, M., Bilde, M., and Ehn, M.: Effect of temperature on the formation of Highly-oxygenated Organic Molecules (HOM) from alpha-pinene ozonolysis, Atmos. Chem. Phys. Discuss., https://doi.org/10.5194/acp-2018-1276, in review, 2018.

Roldin P., Ehn, M, Kurtén, T., Olenius, T., Rissanen, M.P., Sarnela, N., Elm, J., Rantala, P., Hao, L., Hyttinen, N., Heikkinen, L., Worsnop, D. R., Pichelstorfer, L., Xavier, C., Clusius, P., Öström, E., Petäjä, T., Kulmala, M., Vehkamäki, H., Virtanen, A., Riipinen, I., and Boy, M., The role of highly oxygenated organic molecules in the Boreal aerosol-cloud-climate system, Nature Communications, in press 2019.

Rosenfeld, D., Andreae, M. O., Asmi, A., Chin M., De Leeuw, G., Donovan, D. P., Kahn, R, Kinne, S., Kivekäs, N., Kulmala, M.,, Lau W., Schmidt K, S., Suni T., Wagner T., Wild, M., and Quaas J., Global observations of aerosol-cloud-precipitation-climate interactions,Rev. Geophys.,52,750–808, doi:10.1002/2013RG000441.

Rissanen, M. P., Kurtén, T., Sipilä, M., Thornton, J. A., Kausiala, O., Garmash, O., Kjaergaard, H. G., Petäjä, T., Worsnop, D. R., Ehn, M. and Kulmala, M.: Effects of chemical complexity on the autoxidation mechanisms of endocyclic alkene ozonolysis products: From methylcyclohexenes toward understanding α-pinene, J. Phys. Chem. A, 119(19), 4633–4650, doi:10.1021/jp510966g, 2015.

Saathoff, H. and Naumann, K.-H.: Temperature dependence of yields of secondary organic aerosols from the ozonolysis of α-pinene and limonene, Atmos. Chem. Phys., (March), 4–15, doi:10.5194/acp-9-1551-2009, 2009.

Sarrafzadeh, M., Wildt, J., Pullinen, I., Springer, M., Kleist, E., Tillmann, R., Schmitt, S. H., Wu, C., Mentel, T. F., Zhao, D., Hastie, D. R. and Kiendler-Scharr, A.: Impact of NOxand OH on secondary organic aerosol formation from β-pinene photooxidation, Atmos. Chem. Phys., 16(17), 11237–11248, doi:10.5194/acp-16-11237-2016, 2016.

Saunders, S. M., Jenkin, M. E., Derwent, R. G. and Pilling, M. J.: Protocol for the development of the Master Chemical Mechanism, MCM v3 (Part A): Tropospheric degradation of non-aromatic volatile organic compounds, Atmos. Chem. Phys., 3(1), 161–180, doi:10.5194/acp-3-161-2003, 2003.

Schmale, J., Henning, S., Henzing, B., Keskinen, H., Sellegri, K., Ovadnevaite, J., Bougiatioti, A., Kalivitis, N., Stavroulas, I., Jefferson, A., Park, M., Schlag, P., Kristensson, A., Iwamoto, Y., Pringle, K., Reddington, C., Aalto, P., Äijälä, M., Baltensperger, U., Bialek, J., Birmili, W., Bukowiecki, N., Ehn, M., Fjæraa, A. M., Fiebig, M., Frank, G., Fröhlich, R., Frumau, A., Furuya, M., Hammer, E., Heikkinen, L., Herrmann, E., Holzinger, R., Hyono, H., Kanakidou, M., Kiendler-Scharr, A., Kinouchi, K., Kos, G., Kulmala, M., Mihalopoulos, N., Motos, G., Nenes, A., O'Dowd, C., Paramonov, M., Petäjä, T., Picard, D., Poulain, L., Prévôt, A. S. H., Slowik, J., Sonntag, A., Swietlicki, E., Svenningsson, B., Tsurumaru, H., Wiedensohler, A., Wittbom, C., Ogren, J. A., Matsuki, A., Yum, S. S., Myhre, C. L., Carslaw, K., Stratmann, F. and Gysel, M.: Corrigendum: Collocated observations of cloud condensation nuclei, particle size distributions, and chemical composition, Sci. data, 5, 180094, doi:10.1038/sdata.2018.94, 2018.

Shilling, J. E.: Particle mass yield in secondary organic aerosol formed by the dark ozonolysis of α-pinene, Atmos. Chem. Phys., 8(1992), 2073–2088, 2008.

Stirnweis, L., Marcolli, C., Dommen, J., Barmet, P., Frege, C., Platt, S. M., Bruns, E. A., Krapf, M., Slowik, J. G., Wolf, R., Prévôt, A. S. H., Baltensperger, U. and El-Haddad, I.: Assessing the influence of NOx concentrations and relative humidity on secondary organic aerosol yields from α-pinene photo-oxidation through smog chamber experiments and modelling calculations, Atmos. Chem. Phys., 17(8), 5035–5061, doi:10.5194/acp-17-5035-2017, 2017.

Tasoglou, A. and Pandis, S. N.: Formation and chemical aging of secondary organic aerosol during the β-caryophyllene oxidation, Atmos. Chem. Phys., 15(11), 6035–6046, doi:10.5194/acp-15-6035-2015, 2015.

Topping, D.: UManSysProp v1.0: an online and open-source facility for molecular property prediction and atmospheric aerosol calculations, , 899–914, doi:10.5281/zenodo.45143, 2016.

Waring, M. S.: Secondary organic aerosol formation by limonene ozonolysis: Parameterizing multi-generational chemistry in ozone- and residence time-limited indoor environments, Atmos. Environ., 144, 79–86, doi:https://doi.org/10.1016/j.atmosenv.2016.08.051, 2016.

Zhao, D., Schmitt, S. H., Wang, M., Acir, I. H., Tillmann, R., Tan, Z., Novelli, A., Fuchs, H., Pullinen, I., Wegener, R., Rohrer, F., Wildt, J., Kiendler-Scharr, A., Wahner, A. and Mentel, T. F.: Effects of NOx and SO2 on the secondary organic aerosol formation from photooxidation of α-pinene and limonene, Atmos. Chem. Phys., 18(3), 1611–1628, doi:10.5194/acp-18-1611-2018, 2018.

Zhao, D. F., Kaminski, M., Schlag, P., Fuchs, H., Acir, I. H., Bohn, B., Häseler, R., Kiendler-Scharr, A., Rohrer, F., Tillmann, R., Wang, M. J., Wegener, R., Wildt, J., Wahner, A. and Mentel, T. F.: Secondary organic aerosol formation from hydroxyl radical oxidation and ozonolysis of monoterpenes, Atmos. Chem. Phys., 15(2), 991–1012, doi:10.5194/acp-15-991-2015, 2015.

Supplement material

Table 1s(a). List of compounds contributing to > 95% of SOA mass yield at 258K. The names of compounds are given in MCM format. The PRAM compounds are highlighted in red.

Molecular Weight (g/mol)	Species name	Contribution (%)
430	C20H30O10	0.16
198	C10H14O4	0.17
462	C20H30O12	0.18
214	C10H14O5	0.18
174.19	C810OOH	0.19
178.14	C621OOH	0.19
277	C10H15O8N1	0.19
130.1	H1C23C4CHO	0.2
341	C10H15O12N1	0.21
203.19	C810NO3	0.22
446	C20H30O11	0.22
293	C10H15O9N1	0.24
309	C10H15O10N1	0.24
312	C10H16O11	0.24
206.19	C813OOH	0.25
190.19	C812OOH	0.26
170.21	C89CO2H	0.28
174.19	C811OOH	0.29
188.22	C920OOH	0.29
220.22	C922OOH	0.3
204.22	C921OOH	0.3
310	C10H14O11	0.32
325	C10H15O11N1	0.33

235.19	C813NO3	0.36
294	C10H14O10	0.52
230	C10H14O6	0.55
203.19	C811NO3	0.56
296	C10H16O10	0.58
262	C10H14O8	0.65
280	C10H16O9	0.84
246	C10H14O7	0.88
278	C10H14O9	0.93
264	C10H16O8	1.11
248	C10H16O7	1.12
232	C10H16O6	1.13
216	C10H16O5	1.23
172.22	C96OOH	1.32
200	C10H16O4	1.39
162.14	C614OOH	1.64
191.14	C614NO3	2.49
204.22	C98OOH	2.88
188.22	C97OOH	3.07
174.15	C717OOH	3.43
184.23	PINONIC	4.4
233.22	C98NO3	4.53
200.23	C109OOH	4.75
216.23	C108OOH	5.67
200.23	C107OOH	5.94
245.23	C108NO3	8.97
261.23	C920PAN	9.35

247.2	C811PAN	10.11
203.15	C717NO3	11.29

1202
1203

1204 **Table 1s(b)**. List of compounds contributing to > 95% of SOA mass yield at 293K. The names of compounds
1205 are given in MCM format.

Molecular Weight (g/mol)	Species names	Contribution (%)
496	C19H28O15	0.45
174.15	C717OOH	0.53
344	C10H16O13	0.57
446	C20H30O11	0.59
448	C19H28O12	0.62
248	C10H16O7	0.67
200.23	HOPINONIC	0.7
462	C20H30O12	0.7
480	C19H28O14	0.76
186.21	PINIC	0.77
188.22	C920OOH	0.79
510	C20H30O15	0.79
325	C10H15O11N1	0.8
464	C19H28O13	0.82
373	C10H15O14N1	0.9
178.14	C621OOH	1.03
478	C20H30O13	1.1
246	C10H14O7	1.17
341	C10H15O12N1	1.2
262	C10H14O8	1.26
174.19	C811OOH	1.35

494	C20H30O14	1.39
164.11	C516OOH	1.44
245.23	C108NO3	1.49
162.14	C614OOH	1.6
220.22	C922OOH	1.64
200	C10H16O4	1.65
204.22	C921OOH	1.68
357	C10H15O13N1	1.93
264	C10H16O8	1.97
328	C10H16O12	2.2
280	C10H16O9	2.35
326	C10H14O12	2.41
206.19	C813OOH	2.64
190.19	C812OOH	2.73
312	C10H16O11	2.77
278	C10H14O9	2.86
188.22	C97OOH	3.03
235.19	C813NO3	3.1
296	C10H16O10	3.19
294	C10H14O10	3.63
233.22	C98NO3	3.81
261.23	C920PAN	4.1
247.2	C811PAN	4.57
310	C10H14O11	6.19
216.23	C108OOH	6.24
204.22	C98OOH	7.44

Table 1s(c). List of compounds contributing to > 95% of SOA mass yield at 313K. The names of compounds are given in MCM format.

Molecular Weight (g/mol)	Species names	Contribution (%)
526	C20H30O16	0.54
512	C19H28O16	0.55
450	C18H26O13	0.56
482	C18H26O15	0.6
280	C10H16O9	0.6
294	C10H14O10	0.7
466	C18H26O14	0.79
296	C10H16O10	0.9
278	C10H14O9	1
464	C19H28O13	1.2
204.22	C98OOH	1.42
344	C10H16O13	1.51
496	C19H28O15	1.65
480	C19H28O14	1.77
178.14	C621OOH	1.93
373	C10H15O14N1	1.95
510	C20H30O15	2.57
204.22	C921OOH	3.03
494	C20H30O14	3.15
220.22	C922OOH	3.26
164.11	C516OOH	3.85
357	C10H15O13N1	4.63
312	C10H16O11	5.62
326	C10H14O12	6.04

328	C10H16O12	6.56
235.19	C813NO3	6.83
190.19	C812OOH	6.95
206.19	C813OOH	7.46
310	C10H14O11	18.28

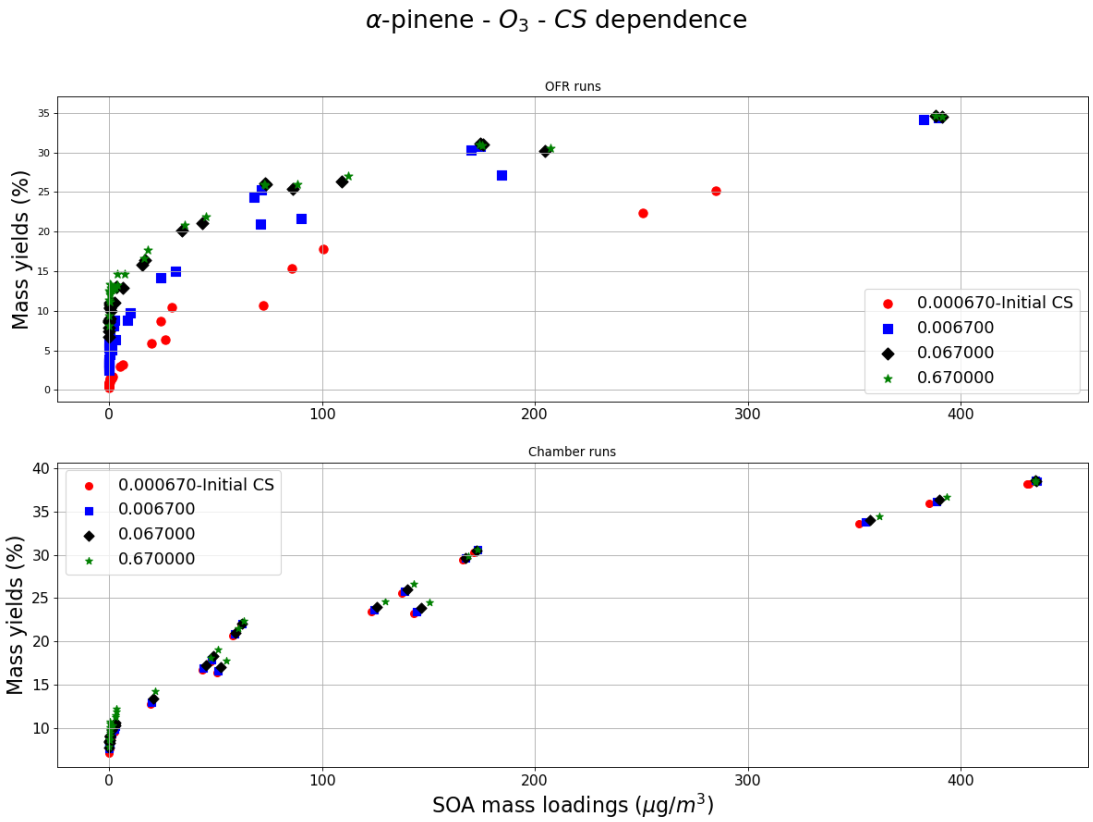

Figure S1. SOA mass yields for α-pinene oxidation using O_3 for different CS values. For the OFR runs the yields level off above a CS value of 0.067 s^{-1} , while chamber simulation show negligible variation with CS . Hence 0.067 s^{-1} is selected as CS for the OFR simulations while chamber simulations are run with 0.00067 s^{-1}.

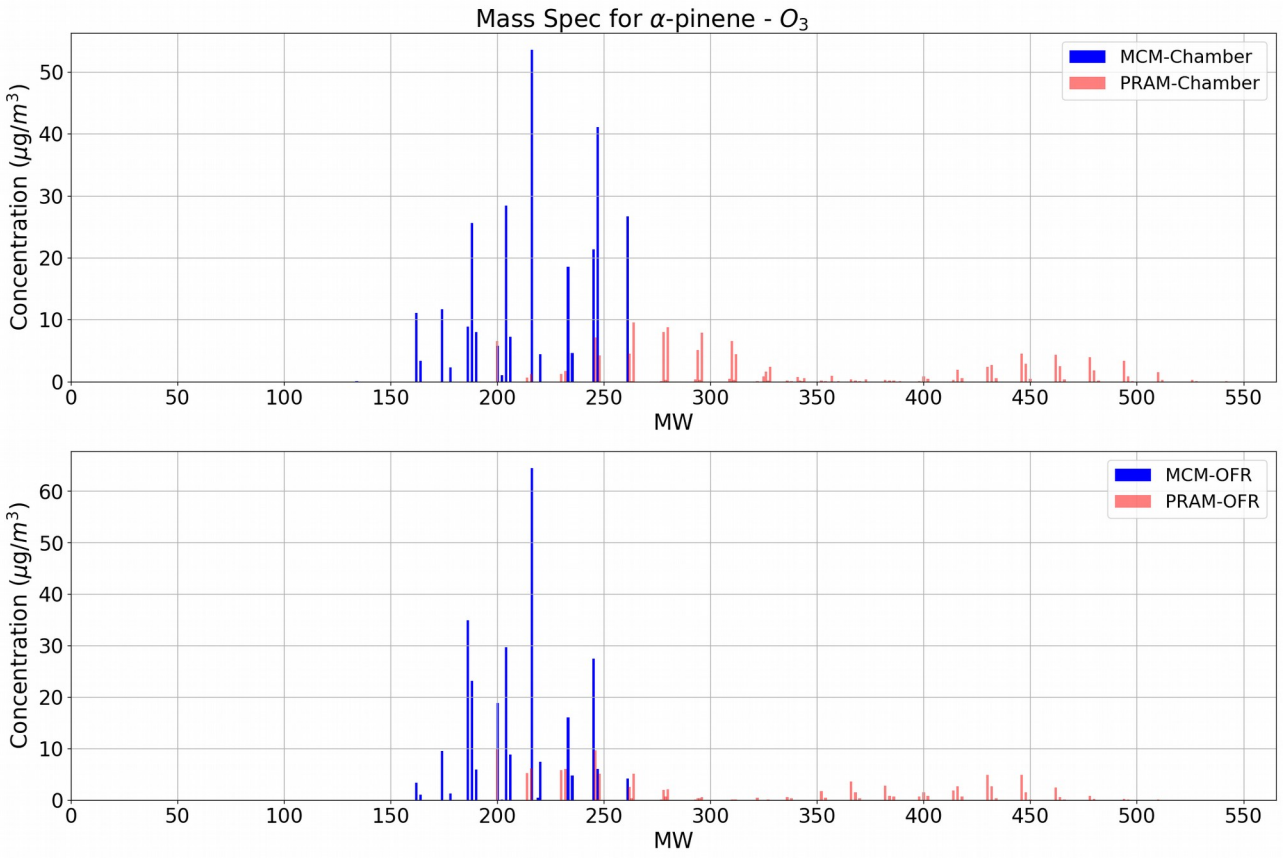

Figure S2. Mass spectra of SOA formed from α-pinene ozonolysis in the particle phase. The upper panel indicates spectra from chamber simulations while the lower panel represents the spectra from OFR simulations.

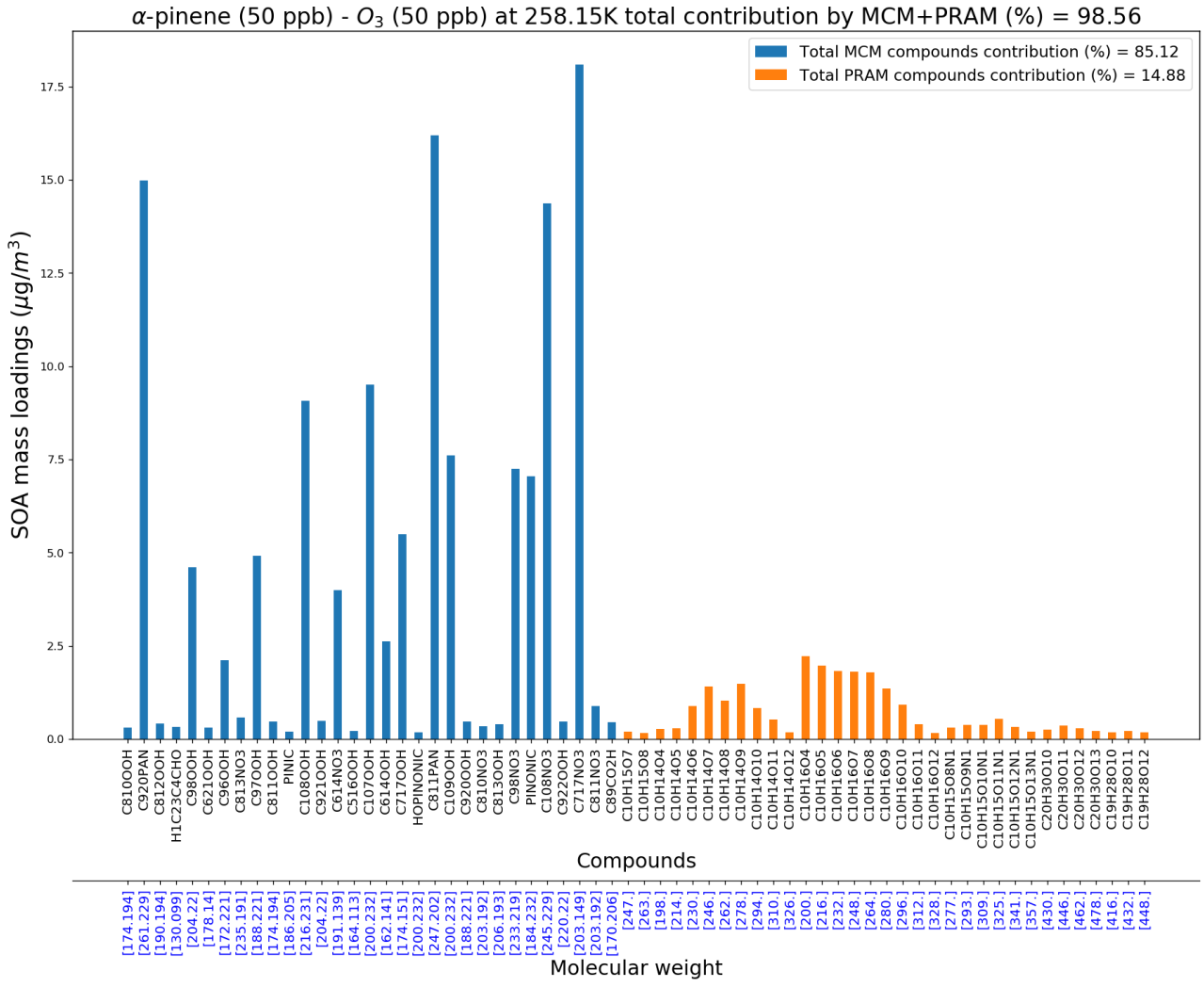

Figure S3(a). MCM and PRAM compounds contributing to > 95% of SOA mass at 258 K and 50ppb O_3 and α-pinene concentrations. It can be noted that a large fraction of the PRAM species that contribute to the SOA mass at 258 K are not classified as HOM (i.e. contain at least 6 oxygen atoms), and many of them will not be detected in the gas-phase using the present state-of-the-art Chemical Ionization-Atmospheric Pressure Interface TOF (CI-APi-TOF) technique.

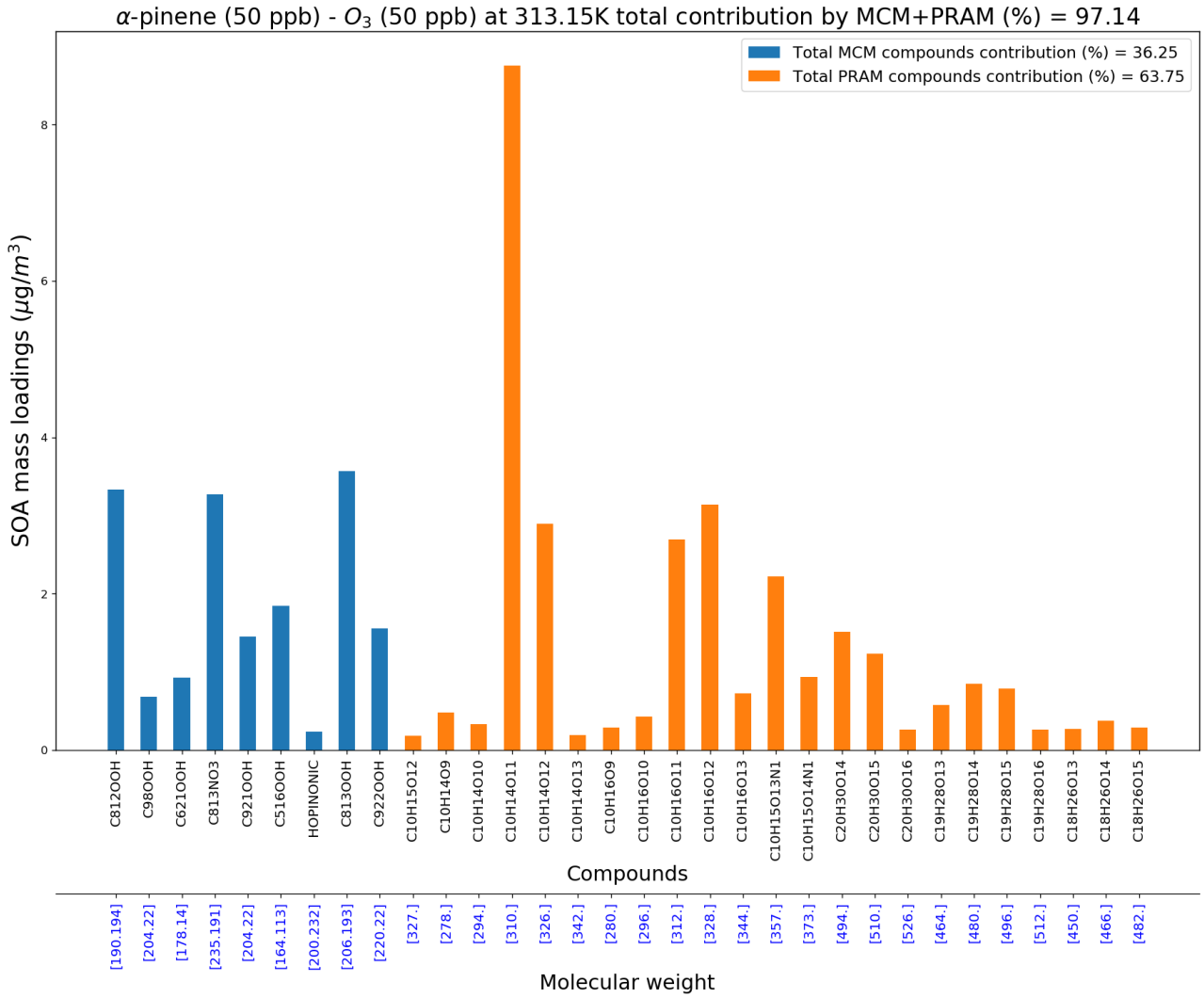

Figure S3(b). MCM and PRAM compounds contributing to > 95% of SOA mass at 313.15 K and 50ppb O_3 and α-pinene concentrations.

The importance of using the MCM+PRAM scheme is illustrated in Fig. 4 which shows the relative contribution by PRAM and MCM compounds for the oxidation of α -pinene, β-pinene and limonene by OH (upper panel) and O_3 (lower panel) for their respective maximum SOA mass yields for both chamber and flow tube setup simulations. The present PRAM mechanism does not include the peroxy radical autooxidation products from β-pinene ozonolysis, products from oxidation of isoprene and β-caryophyllene and the products from NO_3 oxidation of BVOCs. Therefore, they are excluded from Fig.4.

The impact of PRAM compounds contribution to limonene ozonolysis, irrespective of chamber or flow tube setup is considered. It is evident from Fig. 9 (lower panel), which shows that upon using the standalone MCM mechanism underpredicts the SOA mass yields with PRAM compounds contributing ~ 80% and 60% respectively. For α-pinene ozonolysis, the standalone MCM scheme under-predicts the modelled mass yields by approximately 25 % and 22.5 % respectively.

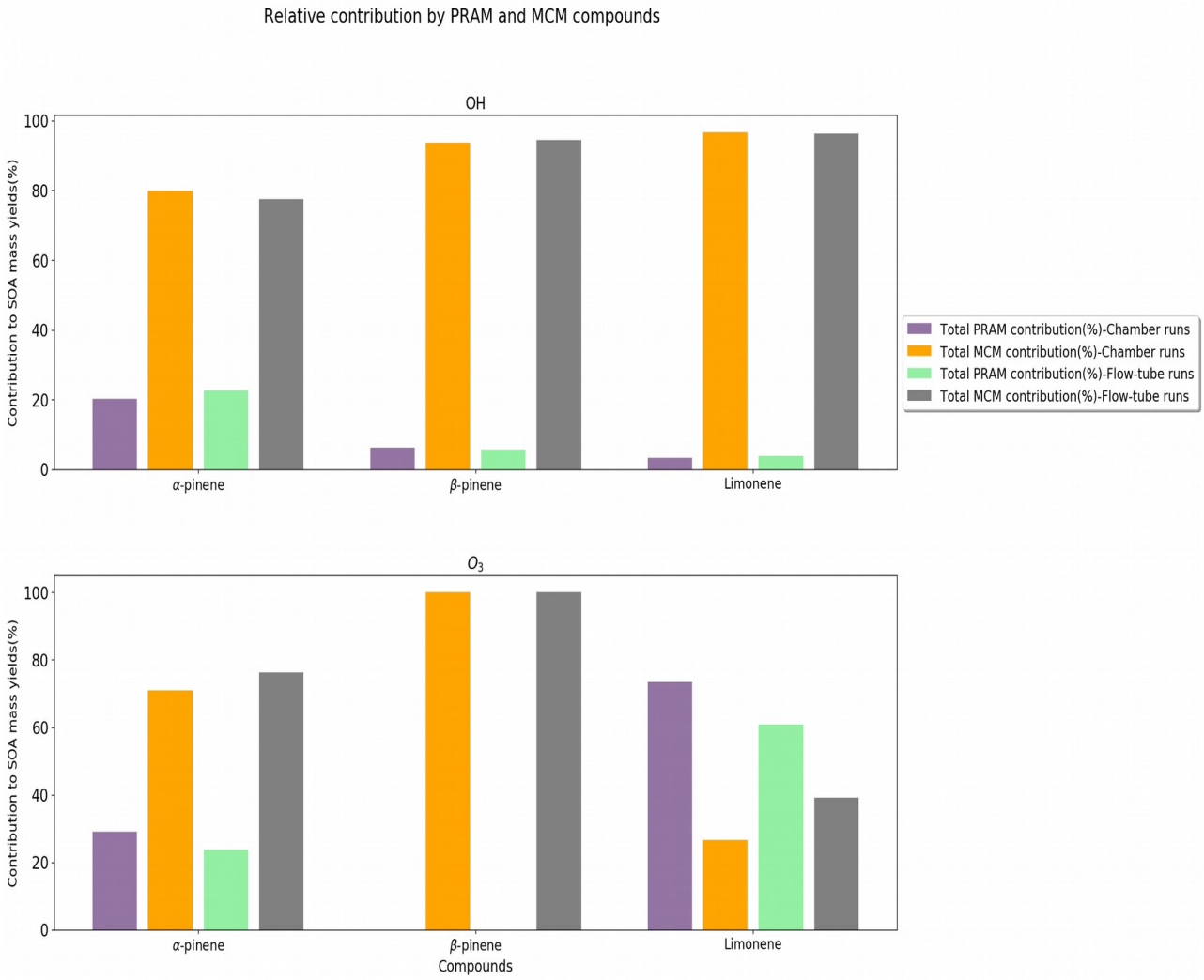

Figure 4. Relative contribution of HOM and MCM compounds for selected maximum mass yields of α- pinene, β-pinene and limonene oxidation by OH (upper panel) and O_3 (lower panel) at 293.15 K.

Summary of experimental data used for comparison

Kristensen et al., (2017) investigated α-pinene ozonolysis SOA mass yields at temperatures of 258 and 293 K. Additionally SOA mass yields from OH oxidation of α-pinene were also investigated. Yields for α-pinene at higher temperatures of 313 K were investigated by Pathak et al., (2007), wherein they performed experiments using ammonium sulfate seed particles. Shilling et al., (2008) performed experiments for lower concentrations of α-pinene ozonolysis combinations and hence used to compare yields for loading's < 10 μg m^{-3} . Griffin et al., (1999) used smog chambers to investigate the aerosol forming potential of various BVOCs such as β-pinene by ozonolysis and β-caryophyllene by OH oxidation. The SOA mass yields derievd from the OH oxidation of isoprene, β-caryophyllene and β-pinene were experimented by Lee et al., (2006b).

The SOA mass yields derived from the ozonolyis of α-pinene and limonene using an OFR were compared with the experimental yield from Kang and Root, (2007). The experiments also provided estimates on SOA mass yields underestimation when performed with/without acidic seed particles in the OFR. Yields simulated from the OH oxidation of α-pinene were compared against yields measured by (Bruns et al., 2015) as they had used similar initial BVOC and oxidant concentrations. The simulated yields were also compared with experimental yields from Friedman and Farmer, (2018) due to similar initial oxidant concentrations used.